

## ABSTRACT

LIN, TIANHENG. Development and Testing of Ammonia – Oxygen Monitoring System for Poultry Houses. (Under the direction of Dr. Sanjay B. Shah).

High ammonia concentrations and low oxygen concentrations in poultry houses can adversely impact bird performance; hence it is important to monitor the concentrations of these gases. Handheld ammonia measurement methods, such as, pH test paper, gas tube, and electrochemical (EC) sensor have advantages, but also disadvantages that have limited their large-scale adoption. A low-cost and portable ammonia - oxygen measurement system would be very useful to poultry producers. Three brands of ammonia metal oxide semiconductor (MOS) sensors were compared, and Figaro TGS2444 sensor was selected due to its superior performance. Temperature and relative humidity (RH) compensation equations were used to account for sensor responses as affected by changes in those parameters. The ammonia sensors were tested with synthetic ammonia gas mixture and air exhausted from a chamber containing poultry litter in realistic ranges of ammonia concentration, RH, and temperature. Compared with the highly-accurate acid scrubber, averaged over 13 measurement events, relative error and coefficient of variation of the MOS sensor were 8.8% and 6.6%, respectively. The MOS sensor also performed well against gas tubes and the electrochemical sensor. Of the two electrochemical oxygen sensors evaluated, the Figaro KE-25 was selected based on its superior performance and longer life. The assembled ammonia – oxygen sensor system had a response time of <1 min, its total mass was <1.4 kg, and its material cost was <\$450. Hence this highly portable system could be a cost-effective option for air quality management in poultry houses. Further testing in poultry houses is recommended.

Development and Testing of an Ammonia-Oxygen Monitoring System for Use in Poultry Houses

by  
Tianheng Lin

A thesis submitted to the Graduate Faculty of  
North Carolina State University  
in partial fulfillment of the  
requirements for the Degree of  
Master of Science

Biological and Agricultural Engineering

Raleigh, North Carolina

2015

APPROVED BY:

---

Dr. Sanjay B. Shah  
Committee Chair

---

Dr. Lingjuan Wang Li

---

Dr. Edgar O. Oviedo-Rondón

---

Dr. Justin Blaise Post

## **BIOGRAPHY**

Tianheng Lin was born in Shanghai, China. Tianheng obtained a BS in electrical engineering from Shanghai Normal University in 2011. In Fall 2013, Tianheng enrolled in North Carolina State University to pursue an MS in Biological and Agricultural Engineering.

## **ACKNOWLEDGMENTS**

This study is supported by U.S. Poultry and Egg Association.

I would like to thank Dr. Sanjay Shah, Dr. Lingjuan Wang Li, Dr. Edgar Oviedo-Rondón and Dr. Justin Post for their guidance and help throughout this project.

I would like to thank BAE Department personnel Dr. Praveen Kolar, Phil Harris, Timothy Seaboch, David Buffaloe, Neil Bain, Craig Baird, and Rachel Huie for the valuable technical support for the project.

Thanks also go to Steven Turnage, Kathleen Giedraitis and Yuting Zheng for their help with lab testing.

Last but not least, I would like to thank my family for their insistence and kindness throughout my life.

**TABLE OF CONTENTS**

**LIST OF TABLES** ..... vi

**LIST OF FIGURES** ..... vii

**1. Introduction**..... 1

**1.1. Broiler and turkey production in North Carolina** ..... 1

**1.2. Ammonia and oxygen concentrations in poultry houses**..... 1

**1.3. Recommendations for ammonia and oxygen concentrations in poultry houses** 2

**1.4. Ammonia and oxygen measurement methods**..... 2

**1.4.1. Ammonia measurement methods** ..... 2

**1.4.2 Oxygen measurement methods** ..... 3

**1.5. Objectives**..... 4

**2. Literature Review** ..... 5

**2.1. Introduction**..... 5

**2.2. Ammonia measurement methods** ..... 5

**2.2.1. pH ammonia test paper** ..... 5

**2.2.2. Scrubbers** ..... 6

**2.2.3. Filter pack**..... 6

**2.2.4. Denuder**..... 7

**2.2.5. Gas tubes**..... 7

**2.2.6. Spectroscopic methods**..... 7

**2.2.7. Chemiluminescence analyzer** ..... 9

**2.2.8. Gas chromatography** ..... 9

**2.2.9. Electrochemical sensor** ..... 10

**2.2.10. Metal oxide semiconductor sensor**..... 10

**2.2.11. Conductive polymers sensor**..... 11

**2.2.12. Surface acoustic wave sensor** ..... 12

**2.2.13 Quartz crystal microbalance sensor**..... 12

**2.2.14. Summary of ammonia monitoring methods**..... 13

**2.3 Oxygen monitoring methods**..... 15

2.4	MOS sensor for ammonia measurement.....	15
2.4.1.	Working principle .....	15
2.4.2.	Influencing factors .....	17
2.4.3.	Mitigation methods .....	17
2.5.	Summary of literature review .....	18
3.	Material and Methods .....	19
3.1.	Ammonia sensor testing.....	19
3.1.1.	Comparison of ammonia sensors.....	19
3.1.2.	Ammonia sensor calibration .....	24
3.1.3.	Sensor testing with poultry litter chamber exhaust .....	27
3.2	Oxygen sensor testing .....	30
3.3	Sensor system fabrication.....	31
3.3.1	Data acquisition, control, and display .....	31
3.3.2	System assembly.....	31
3.3.3	Power supply .....	33
3.4	Fabricated units testing.....	34
3.5.	Ancillary considerations .....	36
4.	Results and discussion .....	38
4.1.	Ammonia sensor testing.....	38
4.1.1.	Comparison of ammonia sensors.....	38
4.1.2.	Ammonia sensor calibration .....	41
4.1.3.	Poultry litter chamber testing of ammonia sensor.....	54
4.1.4	Testing of the assembled units.....	59
4.2	Oxygen sensor testing .....	63
	REFERENCES.....	68

## LIST OF TABLES

Table 2.1. Summary of ammonia detection methods.....	14
Table 3.1. Make, price, and measurement range of the three MOS ammonia sensors .....	19
Table 3.2. Flow rates and ammonia concentrations for comparing the three ammonia sensors .....	23
Table 3.3. Flow rates and ammonia concentrations for sensor calibration .....	25
Table 3.4. Flow rates and oxygen concentrations used for oxygen sensor comparison .....	30
Table 3.5. List of components used in the ammonia – oxygen sensor system and their prices (including shipping and handling). Prices do not include taxes. ....	33
Table 4.1. Quantitative comparison of the three ammonia measurement methods (Drager, scrubber, and MOS/TGS2444 sensor units).....	57
Table 4.4. Responses of the three oxygen sensors and their respective RH and temperature sensors to ambient condition (30.3-30.8 °C and 37.5-50.1% RH). Ambient temperature and RH were measured with a TMA40-A anemometer equipped with temperature and RH sensors. ....	65

## LIST OF FIGURES

Figure 3.1. One air-stream humidifier set-up. The desiccant used was 3 Å molecular sieve. Tap water was used for humidification. ....	20
Figure 3.2. Data acquisition system and test chamber for lab testing.....	21
Figure 3.3. Voltage divider circuit design. VS is sensor output measured across the loading resistor (RL) and RS is the sensor resistor. ....	22
Figure 3.4. Set-up for comparing the three types of ammonia sensors in the lab.....	22
Figure 3.5. Set-up for calibrating the three TGS2444 sensors.....	26
Figure 3.6. Porous base of the poultry litter chamber. ....	28
Figure 3.7. Chamber testing set-up using poultry litter as the ammonia source.....	29
Figure 3.8. Layout of the oxygen sensor testing system.....	30
Figure 3.9. Lay out of the ammonia - oxygen sensor system .....	32
Figure 3.10. Picture of the assembled sensor system.....	32
Figure 3.11. Layout of the system used to test the fabricated units.....	35
Figure 3.12. Picture of the modified fabricated units testing system for high temperature test. ....	36
Figure 3.13. Picture of hydrophobic filter installed in the sensor chamber .....	37
Figure 4.1. Analog outputs of the three MOS ammonia sensors at 26 °C to 29 °C and 43% RH to 35% RH. Each trend line is the output of a single sensor. The three sensors are: FIS SP-53B, SGX MiCS 5914, and Figaro TGS2444. Sensor readings were scanned and recorded every 5 s. ....	38
Figure 4.2. Response of one Figaro TGS2444 sensor to changes in ammonia concentrations and RH conditions. The sensor was not tested at high RH at 5 and 15 ppm ammonia concentrations. Each data point is based on an average of five readings. ....	39
Figure 4.3. Response of one FIS SP-53B sensor to changes in ammonia concentrations and RH conditions. The sensor was not tested at high RH at 5 and 15 ppm ammonia concentrations. Each data point is based on an average of five readings. ....	40
Figure 4.4. Response of one SGX MiCS 5914 sensor to changes in ammonia concentrations and RH conditions. The sensor was not tested at high RH at 5 and 15 ppm ammonia concentrations. Each data point is based on an average of five readings. ....	40
Figure 4.5. Relationship between chamber RH and fraction of humidified air in the two air-stream humidifier as measured with the CS 500 temperature/RH sensor. Each data point is based on an average of five readings. ....	41
Figure 4.6. Change in test chamber RH for different proportions of the humidified and dry air-stream. Total airflow rate was 4-6 L/min and the testing was performed in a temperature range of 24.6 °C to 25.1 °C with a room RH of 55%. Readings were taken every 5 s. ....	42
Figure 4.7. Response of one TGS2444 sensor to 25 ppm ammonia concentration at three airflow rates (1, 3, and 5 L/min). The sampling and purging time was 5 min. This study was	

conducted at a temperature of 25 °C and 61% RH. Readings were taken every 5 s. ....	43
Figure 4.8. Response of one TGS2444 sensor to 25 ppm ammonia concentration at three airflow rates (1, 2, and 3 L/min). The sampling and purging time was 5 min. This study was conducted at a temperature of 26 °C and 59% RH. Readings were taken every 5 s. ....	44
Figure 4.9. Response of one TGS2444 sensor to alternating 25 and 50 ppm ammonia concentration with 3 min of exposure at each concentration (fixed RH of ~62% and temperature of 22 °C). Readings were taken every 5 s. ....	45
Figure 4.10. Short-term drift of one TGS2444 ammonia sensor at nominal ammonia concentration of 25 ppm (fixed RH of ~62% and temperature of 22 °C). Each data point is a measurement taken at 5-s intervals. ....	46
Figure 4.11. Comparison of the three LM34 temperature sensors in the lab. Temperature readings were taken every 5 s. ....	47
Figure 4.12. Adjusted LM34 temperature sensors outputs. ....	47
Figure 4.13. Comparison of three HIH-4000-003 RH sensors in the lab. Readings were taken every 5 s. ....	48
Figure 4.14. Responses of three Figaro TGS2444 sensors to changing ammonia concentrations (5-50 ppm) under low (55%) and high (80%) RH conditions. Measurements were taken every 5 s. Test temperature was ~25 °C. ....	49
Figure 4.15. Responses (n = 40) of (a) MOS1, (b) MOS2, and (c) MOS3 sensors to ammonia concentrations (5-50 ppm) at low and high RH conditions. Test temperature was ~25 °C. ...	51
Figure 4.16. Mean of MOS1, MOS2, and MOS3 sensor outputs as a function of ammonia concentration and RH at 25 °C. Each data point is the sensor's mean and the error bars are SD values. The mean of each sensor's output is based on five measurements taken at 5-s intervals. ....	52
Figure 4.17. Comparison of ammonia concentrations in air exhausted from a chamber containing poultry litter measured with MOS sensor units, Drager EC sensor, and gas tube at 20 °C (58-63% RH) and 30 °C (40-45% RH). For each event, average Drager ammonia concentration is based on 10 readings while the average reading for each MOS sensor is based on 15 readings. The MOS sensors used their individual compensation equations. ....	59
Figure 4.18. Comparison of poultry litter exhaust air ammonia concentrations measured with MOS sensor units and Drager EC sensor at 30 °C. Drager ammonia concentration is based on 10 readings while the average reading for each MOS sensor is based on 15 readings. All MOS sensors used eq. [4.5] for temperature and RH compensation. The average reading for the three MOS sensor units and EC sensor is 35 and 37 ppm, respectively. ....	61
Figure 4.19. Comparison of ammonia concentrations in air exhausted from a chamber containing poultry litter measured with MOS sensor unit (UNIT2, eq. [4.4]) and Drager EC sensor under changing temperature conditions from 20 °C (57% RH) to 30 °C (30% RH). Drager ammonia concentration is based on 10 readings while the average reading for each	

MOS sensor is based on 15 readings. .... 62  
Figure 4.20. Responses of one KE25 and one SGX4 sensor to 17, 19, and 21% oxygen  
concentration at 43% RH and 25.1 °C. Measurements were made every 5 s..... 63

## **1. Introduction**

Ammonia is present in very low concentrations (0.2 ppb-1.5 ppb) in ambient air (Sather et al, 2008), but in poultry houses, it is an important pollutant. High ammonia concentrations can decrease bird performance and affect the workers' health. Due to these reasons, ammonia monitoring has received considerable attention, and numerous methods have been developed and are in use for ammonia measurement.

### **1.1. Broiler and turkey production in North Carolina**

North Carolina (NC) is the largest meat producing state in the United States. In 2012, NC ranked No. 4 in broiler production (795 million heads) and No. 2 in turkey production (28.5 million heads) (USDA NASS, 2015). These two commodities combined, accounted for close to half of the farm gate value generated by North Carolina agriculture.

In the last several decades, small family farms were replaced with highly specialized animal farms with greater productivity. Use of modern engineering, science, and management techniques allowed changes in the structure of the animal production system, leading to vertical integration, which made confined livestock agriculture more productive. However, concentrating a large number of animals in a small location also results in large amounts of waste being generated which also causes problems of air quality, particularly, due to ammonia. Sub-optimal oxygen levels due to high stocking densities can also be a concern for bird performance.

### **1.2. Ammonia and oxygen concentrations in poultry houses**

In poultry houses, ammonia is produced naturally due to decomposition of feces and spilled feed. In high concentrations, ammonia can cause irritation to animals' eyes, skin and feet, and thereby, increase the risk of infectious and respiratory diseases (Blake and Hess, 2001). Thus, high concentrations of ammonia can adversely effects their feed conversion, carcass quality, and mortality (Aviagen, 2009).

During brooding and winter time, some farmers reduce ventilation to save energy and this could increase ammonia and decrease oxygen levels. Meanwhile, burning propane or natural gas to provide supplemental heat consumes oxygen (Czarick and Fairchild, 2002). In mountainous areas, reduced oxygen levels (vs. sea level) can further increase respiratory

stress on the birds. In commercial broilers, fast growth and cool temperatures will increase the metabolic requirement for oxygen, forcing the heart to increase its cardiac output (Vogel and Sturkie, 1963). Besch and Kadono (1978) reported that chicken were not able to fully oxygenate their hemoglobin below 15% oxygen. Restoring oxygen concentration to acceptable levels can be achieved by increasing ventilation rate. But excessive ventilation will increase energy use and pollutant gas emissions.

Ammonia is also one of the most important pollutant gases in the environment. Ammonia is the precursor for secondary particulate matter which is harmful to public health and can decrease visibility. Crop and fish production can be reduced due to the soil acidification and eutrophication caused by ammonia deposition (Galloway, 1998).

### **1.3. Recommendations for ammonia and oxygen concentrations in poultry houses**

The National Institute for Occupational Safety and Health (NIOSH) has established a time-weighted average (TWA) exposure limit of 25 ppm for ammonia over an 8-h period and 35 ppm as a 15-min short-term exposure limit (STEL) for humans (NIOSH, 1992). For poultry production, the National Chicken Council (NCC, 2014) set a limit of 25 ppm ammonia at bird height. However, Blake and Hess (2001) recommended that ammonia concentration should be controlled under 10 ppm to ensure bird health. In their animal welfare standards for broiler chickens, the American Humane Association (2012) recommended that ideally, ammonia concentrations should be under 10 ppm with an upper limit of 25 ppm.

Oxygen concentration in the ambient air is approximately 20.95%, while OSHA sets a minimum limit of 19.5% for humans. Once oxygen concentration decreases to 17%, the resulting faster and deeper breathing reduces the poultry's performance, and lower levels of oxygen can threaten the bird's life (Czarick and Fairchild, 2002).

### **1.4. Ammonia and oxygen measurement methods**

#### **1.4.1. Ammonia measurement methods**

Many ammonia measurement methods have been developed and used in livestock barns. Wet chemistry methods were first used in animal facilities by Moum et al. (1969) but such methods do not provide real-time ammonia concentrations. Other chemical methods, such as,

colorimetric (pH) test paper and gas detection tubes provide real-time measurements but these methods are not sufficiently accurate and in the case of gas tubes, not economical (~\$4-8/tube plus a \$200 pump).

Research-grade ammonia detection methods, such as, photoacoustic analyzer (PAS), gas chromatograph mass spectrometer (GC-MS), Fourier transform infrared (FTIR) spectroscopy, differential optical absorption spectroscopy (DOAS), and chemiluminescence (CL) analyzers can be very accurate. However, these methods are expensive, fragile, and not portable enough for use in animal houses for management purposes.

Electrochemical (EC) sensors, including those for ammonia measurement are primarily safety devices, i.e., to ensure that gas concentrations do not reach dangerous levels. Gates et al. (2005) developed a sensor system using the EC ammonia sensor for use in livestock barns for research. While the EC sensor is highly portable and not as expensive as research-grade sensors, they suffer from saturation problems and are more expensive than other methods used for ammonia management (EC detector base unit, \$450; sensor, >\$300).

There are other ammonia sensing technologies that could be suitable for monitoring poultry house ammonia concentrations. One promising design is the wall-mounted optical sensor developed by Lumense (2013) which is suitable for continuous operation. The advantage of the wall-mounted system is the continuous measurement ability which can provide more information, but it is not as convenient as portable devices for random spot measurements.

Metal oxide semiconductor (MOS) ammonia sensors were developed for industrial applications but do have the potential to be used in other areas. Kawashima and Yonemura (2001) first used an MOS ammonia sensor to monitor ambient ammonia concentration near a livestock facility. However, the MOS sensor is sensitive to several environmental factors. But compared to other methods, the MOS sensor has some advantages, e.g., low cost, short response time, compact size, light weight, and long lifetime which makes the MOS sensor a promising candidate for use in a hand-held ammonia sensor system.

#### **1.4.2. Oxygen measurement methods**

Oxygen plays an important role in the field of combustion engines, industrial boilers,

biological, food and chemical processing. Depending on working temperature, oxygen sensors can be classified into high or ambient temperature type. Potentiometric, amperometric, and semiconductor based sensors are three major methods for high temperature oxygen concentration measurement. Galvanic cell, aqueous electrochemical cells, paramagnetic, and optical sensors are suitable for measuring oxygen in ambient temperatures (Ramamoorthy et al., 2003; Weppner, 1992). In the ambient temperature category, the paramagnetic sensor offers excellent performance but is fragile. The optical sensor is relatively new but reasonably-priced sensors are not available. The galvanic and electrochemical cell oxygen sensors are suitable for use in ambient temperatures. These sensors have been in use for decades worldwide, and the maturity of these technologies offer good balance between cost and performance.

No portable, reasonably-priced sensor system that can be used for both ammonia and oxygen measurement could be located. There is need for such a sensor system for managing air quality in poultry houses.

### **1.5. Objectives**

The overall project objective is the development and evaluation of a cost-effective handheld ammonia-oxygen monitoring system for use in poultry houses. This project has the following specific objectives:

1. to select appropriate ammonia and oxygen sensors;
2. to evaluate the performance of the sensors under different conditions in the lab;
3. to fabricate three units of the sensors system; and
4. to evaluate the performance of the units under conditions similar to the field.

The total material cost and mass of the system, preferably, should not exceed \$500 and 1.4 kg (3 lb), respectively. The measurement range for ammonia should be 5-100 ppm, and 15-21% for oxygen. A response time of up to 1 minutes, and relative error less than or equal to 10% would be desirable.

## **2. Literature Review**

### **2.1. Introduction**

Ammonia is a colorless, water-soluble, and reactive gas with a characteristic pungent, suffocating odor. Ammonia is produced naturally due to decomposition of organic matter including plants, animals, and animal wastes (New York State Department of Health, 2004). The Environmental Protection Agency (EPA) prepared an ammonia inventory, which indicated that the poultry sector was the largest contributor among animal husbandry operations (EPA, 2004).

Inside the poultry house, excessive ammonia concentrations can inflame the bird's cornea, burn the skin, and erode its tracheal lining which can lead to respiratory diseases, decreased weight gain, and high mortality (COBB, 2008). Aziz and Barnes (2010) reported that at 7 weeks, compared with broilers raised in 0 ppm ammonia environment, broilers raised in 50 and 75 ppm ammonia environments had 17% and 20% lower body weights, respectively. Similarly, Miles et al. (2004) reported 6 and 9% lower body weights in 50 and 75 ppm ammonia environment, respectively, compared with 0 ppm; mortality at 75 ppm ammonia was 13.9% versus 5.8% in a 0 ppm ammonia environment. Therefore, reliable and regular ammonia monitoring is needed to ensure that cost-effective remediation technologies and practices can be used to improve chicken performance and welfare.

### **2.2. Ammonia measurement methods**

In this chapter, a review of several ammonia measurement methods will be performed. Criteria for assessing gas concentration measurement techniques include: sensitivity, selectivity (specificity), resolution, measurement range, accuracy, precision, sensor life, response time, cost, energy consumption, and adsorptive capacity.

Selection of a sensor or method will depend on the measurement objective (research or management) and operating conditions. Usually, a sensor used for research should have good sensitivity, accuracy, and precision, but for a sensor used for management, high portability, stability, low cost, and short response time could be more important.

#### **2.2.1. pH ammonia test paper**

Moum et al. (1969) first reported using the pH test paper method for measuring ammonia

concentrations in animal facilities. The pH ammonia test paper is the least expensive method (\$0.06/piece), and it has a measurement range of 0-100 ppm with resolution of 5 ppm (Moum et al., 1969). Czarick and Fairchild (2002) reported that pH test paper needed a distilled water supply and its accuracy was poor in the range of 20 to 50 ppm. The advantage of the pH test paper is its on-site measuring capability. The pH test paper method is used by livestock producers to monitor ammonia in their barns. The Chemcassette method is an improvement over the pH test paper as it uses a photo-optical sensor to measure the color change of the pH paper which depends on the sampled gas concentration. A low ammonia concentration Chemcassette has a range of 0.5-30 ppm. The accuracy of the instrument was  $\pm 20\%$  (Bicudo et al., 2000).

### **2.2.2. Scrubbers**

The ammonia scrubber (also called bubbler, trap, or impinger) is a pre-concentration method, in which the ammonia-laden air is passed through an acid solution where an irreversible reaction causes ammonia to be converted to ammonium. The solution is analyzed in the lab for its ammonium concentration and based on the volume of the solution, duration of deployment, and airflow rate through the scrubber, ammonia concentration in the air is determined. The scrubber possesses high efficiency, low detection limit, and is a low-cost method (Shah et al., 2014) but it lacks real-time measurement capability. Using an ion selective electrode to measure ammonium ( $\text{NH}_4^+$ ) concentration in the solution at the site could allow real-time measurements, but the system may be too cumbersome for handheld applications.

### **2.2.3. Filter pack**

The filter pack uses acid-treated filter paper to trap ammonia in air passing through it. A series of filter papers can be used in a filter pack to measure multiple gases. Then the sampled filter is analyzed in the lab. The filter pack has some advantages like low cost, convenient logistics, and particulates sampling capability; they are mainly used for urban ammonia measurement (Shah et al., 2006). But, similar to the scrubber, the filter pack only provides time-weighted concentrations, which make them unsuitable for real-time ammonia monitoring.

#### **2.2.4. Denuder**

Another pre-concentration method is the denuder, in which a tube coated with acid material traps ammonia pulled through it. Then the denuder is analyzed in the lab. Denuders can be separated into passive and active designs. Active denuders require measurement of wind speed while the passive denuders are calibrated in the wind tunnel. Denuders generally provide flow-weighted average or time-weighted average gas concentration (EMEP, 2001; Ferm et al., 2005; Fitz et al., 2003.) and are thus unsuitable for real-time monitoring.

Wyers et al. (1993) developed a continuous-flow denuder, namely, ammonia measurement by annular denuder sampling with on-line analysis (AMANDA). In the continuous-flow denuder, an acid solution in the rotating denuder is used to trap ammonia gas, which is measured using conductometry. It had a measurement range of  $6 \text{ ng m}^{-3}$  to  $1000 \text{ } \mu\text{g m}^{-3}$  with 1-min response time (Mosquera et al., 2002). Its low detection limit and ability to measure in real time make it suitable for ambient ammonia measurement for research purpose, but it is unclear if it can be used in high ammonia concentration environment, such as, the poultry house.

#### **2.2.5. Gas tubes**

The gas tube is a special case of the denuder. A known volume of air is pulled through the tube and ammonia in the air reacts with the medium (phosphoric acid) to cause the medium to change color. Because the length of staining is proportional to the ammonia concentration, it can be directly read on the scale (Meyer and Bundy, 1991). Because no lab analysis or pre-preparation is required, it is very easy to use and suitable for management purposes; gas tubes are widely used by poultry producers for monitoring barn ammonia concentrations. However, it is relatively expensive to use since a single gas tube can cost \$4 to \$8 and it also requires a pump (>\$200). While its relatively low accuracy ( $\pm 15\text{-}18\%$  for  $\leq 50 \text{ ppm}$ ) (RAE Systems, 2001) and precision limits its application in the research field, for management, its accuracy could be considered to be acceptable.

#### **2.2.6. Spectroscopic methods**

Spectroscopic methods are used in ammonia monitoring for research purposes. Most poly-atomic gases exhibit strong vibration-rotation absorption bands in the  $1\text{-}25 \text{ } \mu\text{m}$  region of

the electromagnetic spectrum. Based on the infrared (IR) radiation absorbed by the target gas, the gas concentration can be calculated using Beer-Lambert Law which can be used to predict the concentration of the absorbing species based on the final intensity of the monochromatic radiation (Stuart, 2005).

The non-dispersive infrared (NDIR) sensor is a special case of the IR sensor. Unlike spectrometers, NDIR sensors do not comprise any dispersive optical component but color filters, and only record selected wavelengths (Tury et al., 1991). This method results in lower total price, lower power consumption, and smaller dimension of the detector, and its lifetime is longer.

In the Fourier transform infrared (FTIR) spectroscopy, broadband light is guided through a Michelson interferometer configured with mirrors to produce light beams with different spectrums, for determining the sample's absorbability at each wavelength. The recorded signal with different data points represents the light output as a function of the mirror position, and the raw data is processed by a computer using Fourier transform to calculate the absorption at each wavelength (White, 1989). Harris et al. (2001) used FTIR spectroscopy to measure ammonia emission from a swine finishing operation in North Carolina. Secret (2001) used FTIR to measure air pollutant concentrations near swine feeding operations.

The photoacoustic spectrophotometer (PAS) uses optical filters to provide the optimum wavelength for each gas to maximize absorbance. The target gas heats up when irradiated and cools down as the chopper cuts of the light beam; the resulting change in temperature, and hence, pressure in the measurement chamber is detected by microphones. This acoustic signal is proportional to the concentration of the gas. This instrument has been used to monitor concentrations of several gases in and around swine, poultry, and dairy facilities (Brunsh, 1997; Snell et al., 2003; Zhang et al., 2005; Osada et al., 1998; PAAQL, 2007). Pecen and Zabloudilova (2005) compared the metal oxide semiconductor (MOS) sensor and photoacoustic analyzer for their abilities to measure ammonia concentrations. The PAS is a quick response sensor (30 s for one gas) and it has a wide measurement range (0.2–20,000 ppm) which makes it suitable for both indoor/outdoor gas monitoring.

The ultraviolet differential optical absorption spectroscopy (UV-DOAS) is another device

based on the Beer-Lambert Law. A high-pressure xenon lamp is used as the emitter to project light to the receiver set on the other side of a detection zone. The UV-DOAS was reported to have a relative accuracy between 3.3-11% over the range of 24-200 ppb (Myers et al., 2000). The UV-DOAS's open-path characteristic makes it suitable for measuring gas emission, but the influencing factors present in its light pathway may affect its accuracy.

### **2.2.7. Chemiluminescence analyzer**

The chemiluminescence (CL) ammonia analyzer is an indirect ammonia measurement device. The CL ammonia analyzer contains a converter and an analyzer. The converter converts ammonia to nitric oxide (NO) at 795 °C (eq. [2.1]) (Aneja et al., 1978). In the analyzer, NO is oxidized by O<sub>3</sub> to NO<sub>2</sub> (eq. [2.2]). The NO concentration is proportional to the luminescence produced during its oxidation, which allows for the calculation of ammonia concentration. The CL analyzer has 1 ppb sensitivity, 5 ppb precision, and good linearity (1% full scale), but its cost is high, and its maintenance is relatively complicated (McCulloch and Shendrikar, 2000).



Spectroscopic methods usually have low detection limits (ppb level), low relative error ( $\leq \pm 5.0\%$ ), short response times (seconds to minutes), good selectivity, and real-time ammonia monitoring capability (Vallespi et al., 2013; Tavoli and Alizadeh, 2012; Hu et al., 2012). However, due to their high price, large size, and high power consumption, these methods are suitable only for stationary monitoring.

### **2.2.8. Gas chromatography**

Gas chromatography (GC) is a comprehensive, high-performance chemical analysis instrument. All GCs contain five components: injector, oven, column, detector, and recorder. The liquid, solid, or gaseous sample is introduced into the system by the injector where the solid or liquid sample is evaporated by heating to produce gaseous products. The carrier gas sweeps the sample into the heated column where the sample constituents are separated in the column following the 'like likes like' principle. As the gaseous constituents exit the column, they are counted by the detector (Grob and Barry, 2004). There are several types of detectors,

namely, flame ionization detector (FID), thermal conductivity detector (TCD), electron capture detector (EC), and mass spectrometer (MS). The differences among these detectors are related to their detection range, sensitivity, recoverability, and type of the sample that they can analyze.

The GC-MS is a very versatile instrument which uses the filament current to ionize the gas and accelerate the ions through a charged slit, and then identifies the different components based on their travel time to reach the detector which depends on the masses of the ions (Adams, 2007). The disadvantages of GCs include reduced portability and high cost.

### **2.2.9. Electrochemical sensor**

In an electrochemical sensor, the reduction-oxidation (redox) reactions cause transfer of electrons which can be measured as electric potential (Zhang and Hoshino, 2013). Using this principle, the electrochemical (EC) sensor measures gas concentration based on its current output caused by polarization of the sensing electrode when it react with the oxidizing or reducing gas of interest. Beginning the 1950s, the EC sensor has been used for oxygen monitoring. Due to their superior performance, EC sensors occupy a very big proportion of the gas sensing market.

Gates et al. (2005) developed a portable monitoring unit (PMU) which used an EC sensor to measure ammonia and an IR sensor to measure carbon dioxide in livestock barns. Wheeler et al. (2006) used the PMU to monitor ammonia and CO<sub>2</sub> concentrations in 13 U.S. broiler chicken houses. The main weakness of the EC ammonia sensor is its saturation problem, which can be mitigated by purging for varying durations depending on the EC sensor's model, ammonia concentration and level of use. Another weakness of the EC sensor is its relatively high operating cost because it would have to be replaced quite often depending on the operating conditions. Compared with wet chemistry or IR spectroscopic methods, EC sensors are low-cost, robust, and portable which makes them suitable for industrial ammonia monitoring.

### **2.2.10. Metal oxide semiconductor sensor**

The metal oxide semiconductor (MOS) sensor, when heated, adsorbs oxygen on sensor surface, causing electrons to be drawn from the semiconductor; this results in conversion of

oxygen into an anion, causing an increase in resistance. The target gas (reducing gas), such as, ammonia reacts with the oxygen which decreases sensor resistance; the MOS sensor resistance is proportional to the target gas concentration.

Kawashima and Yonemura (2001) used an MOS sensor for ambient ammonia concentration measurement near livestock facilities. Their MOS sensor had a measurements range from 10 to 100 ppb with 9.7 ppb estimated error. Since the MOS sensor's output increased with relative humidity (RH) linearly, Kawashima and Yonemura (2001) monitored water vapor pressure to adjust the ammonia reading. Pecun and Zabloudivova (2005) compared the MOS sensor with PAS in a poultry litter chamber, and they also noted the influence of RH on the MOS sensor's performance. The MOS sensor has some advantages like low cost, short response time, compact size, and long lifetime, but it is sensitive to environmental factors, especially, moisture.

In the metal oxide semiconductor field effect transistor (MOS-FET), a transistor is used to amplify or switch electronic signals. It can be used as an electronic nose to transform chemical changes into electrical signals. The reaction between the gas-sensitive gate materials (usually, catalytic metals) and certain gases can polarize the catalyst, and therefore, change the threshold voltage (Pearce et al. 2006; Arshak et al. 2004). Ross et al. (1985) reported that Pt gate MOS-FET was sensitive to ammonia. Zhang and Zhao (1989) used Pd-Ir alloy gate MOS-FET for ammonia monitoring. In addition to MOS, FET technology can also be applied to polymer gas sensors. Sarkar et al. (2013) reported that use of polymer-based tunnel field effect transistor (TFET) increased sensitivity to ammonia by more than 10,000 times compared with MOS-FET.

#### **2.2.11. Conductive polymers sensor**

Conductive polymers (CPs) are organic compounds with electrical conductivity that changes when exposed to gases. Phumman et al. (2009) reported that polyphenylene and zeolite composites had negative electrical conductivity responses toward ammonia. Similar to an MOS sensor, a CP sensor also needs doping with redox agents or protonation to improve their sensitivity and selectivity. Several groups of researchers have investigated new types of sensors by mixing polymer with other sensor technologies and have obtained

promising results which will be discussed later.

The carbon nanotube (CNT) is considered to be the ultimate additive for improving electrical properties of structural ceramics. Carbon nanotube based sensors have been found to be quite sensitive to extremely small quantities of gases at room temperature. These sensors can detect extremely low concentrations (ppb) of gases and possess high surface-to-volume ratio, and excellent electrical properties (Kauffman and Star, 2008; Suehiro et al. 2003). Sharma et al. (2013) reported that the multi-walled carbon nanotubes (MWCNTs) were used to reinforce two kinds of polymers, namely, poly (3,4-ethylenedioxythiophene)-poly (styrenesulfonic acid) (PEDOT:PSS) and polyaniline (PANI)). Both sensors were found to have excellent sensitivity and selectivity under room temperature; the MWCNT-PEDOT:PSS exhibited better sensitivity and no drift in its initial resistance value after optimized recovery condition, but their response and recovery time were 15 and 20 min, respectively (Sharma et al., 2013).

#### **2.2.12. Surface acoustic wave sensor**

The surface acoustic wave (SAW) sensors modulate acoustic waves to sense physical phenomena. The SAW chemical vapor sensor uses the thin film polymer coated delay line to select target gas. The absorbed target gas molecules change the acoustic wave time-delay between the input and output electrical signal which is used to determine gas concentration (Ricco et al, 1985). Shen et al. (2004) used L-glutamic acid hydrochloride deposited  $128^\circ$  YX-LiNbO<sub>3</sub> SAW sensor for ammonia measurement. The detection limit was 0.56 ppm, and the degradation rate was 0.01 ppm/day (Shen et al., 2004).

#### **2.2.13. Quartz crystal microbalance sensor**

The quartz crystal microbalance (QCM) sensor measures quartz crystal resonator frequency change to determine the mass change on its surface. Its working principle is similar to the SAW sensor, but the acoustic phase changes inside the quartz crystal, so this sensor is also called the bulk acoustic wave (BAW). Wang et al. (2006) used ZnO nanowires distributed on the quartz crystal surface maintained at  $900^\circ\text{C}$  to measure ammonia. Due to ZnO nanowire's high specific area, fine particle size, and quantum confinement properties, the QCM sensor was considered suitable for gas measurement as it was extremely sensitive

(Wan and Li, 2004). Because the QCM sensor has good stability and reproducibility, it is considered to be suitable in the detection range of 40-100 ppm with 5 s response time.

#### **2.2.14. Summary of ammonia monitoring methods**

The various ammonia monitoring methods are summarized in Table 1. Because the total cost of any method depends on level of use, recalibration frequency, and cost of consumables (e.g., gas tubes) it is difficult to compare the total cost of all the methods.

Spectroscopic methods are very accurate. However, it should be noted that the accuracy provided by the manufacturer is usually based on testing in the optimized lab environment. In the field, test conditions may be considerably more challenging and proper maintenance and accurate calibration may be very difficult. For a short-term research project, the instrument's long-term repeatability may not be a big issue. But for management grade devices, robustness, low-cost, and good stability are very important. Further, instruments used for mobile applications also have to be light and portable.

Several new types of ammonia sensors (e.g., ammonia sensitive polymer or semiconductor materials with CNTs, FET, SAW, or QCM technologies) have been discussed and based on lab results, they seem promising. Unfortunately, these sensors have not been tested in livestock barns that have challenging environments.

There is need for a mobile management grade instrument that can be used by poultry producers for periodic ammonia measurements. As described before, the less-expensive pH paper method provides low accuracy (>10%), the EC sensor has acceptable accuracy but saturates rapidly, and gas tubes can only be used once. All these disadvantages of currently-used measurement methods used in management highlighted the need for sensors, such as, MOS sensors that are low-cost, have short response times, and long lifetimes. As will be discussed in details in Section 2.5, MOS sensor could be useful for poultry house application.

Table 2.1. Summary of ammonia detection methods

Method	Sensitivity	Accuracy	Detection Range	Response Time	Reference
<b>pH test paper</b>	ppm	±20%	0-100 ppm	Seconds	Moum et al. (1969)
<b>Acid scrubber</b>	ppm	±1%	0-1000 ppm	N/A <sup>a</sup>	Shah et al. (2014)
<b>Gas tube</b>	ppm	±10%	0-100 ppm	Minutes	Drager detector tube (Drager Safety, Inc., Pittsburgh, PA)
<b>FTIR</b>	ppb	±5%	N/A	Minutes	Zwicker et al. (1998)
<b>PAS</b>	ppb	±3%	0-500 ppm	Minutes	PAAQL (2007)
<b>IR gas analyzer</b>	ppb	±10%	0-1000 ppm	Minutes	Chillgard RT (Mine Safety Appliances Company, Pittsburgh)
<b>DOAS</b>	ppb	3.3-11%	24-200 ppb	Seconds	Myers et al. (2000)
<b>Continuous-Flow Denuder</b>	ppb	±1%	0.1-1000 ppb	Minutes	Wyers et al. (1993)
<b>CL analyzer</b>	ppb	±1%	0-1000 ppb	Minutes	McCulloch et al. (2000)
<b>Chemcassette</b>	ppm	±20%	0.5-30 ppm	Minutes	Bicudo et al. (2000)
<b>Ammonia electrode</b>	ppb	±2%	0.01-17,000 ppm	Minutes	Orion 9512HPBNWP (Thermo Fisher Sci, Inc., Beverly, MA)
<b>Optical polymer sensor</b>	ppm	N/A	5-300 ppm	Minutes	LE-100 ammonia sensor (Lumense, Inc. Atlanta, GA)
<b>EC sensor</b>	ppm	±3%	0-300 ppm	Minutes	DragerSesnor XS (Drager Safety, Inc., Pittsburgh, PA)
<b>MOS sensor</b>	ppm	±10%	0-100 ppm	Seconds	Krause and Janssen (1990, 1991)
<b>MOS (low conc.)</b>	ppb	±10%	10-100 ppb	Seconds	Kawashima et al. (2001)

<sup>a</sup>Not applicable.

### **2.3. Oxygen monitoring methods**

Oxygen sensors are widely used for workplace air monitoring. Two types of sensors, paramagnetic and electrochemical, are used in portable devices. Oxygen has two unpaired electrons in its outer shell which imparts it with high magnetic characteristic. The paramagnetic oxygen sensor consists of a small dumbbell filled with inert gas and as oxygen is attracted to the magnetic fields the resulting torque on the dumbbell is proportional to the oxygen concentration. Paramagnetic sensors offer excellent precision and response time, but are delicate, expensive, and sensitive to other influencing gases which make them unsuitable for mobile applications (Manning et al., 1999).

The most commonly used oxygen sensors are the electrochemical (EC) sensors. Hanrahan et al. (2004) reported that EC sensors were highly suitable for meeting the size, cost, and power consumption requirements for on-site oxygen monitoring. Walsh et al. (2010) reported that the EC oxygen sensors over-estimated oxygen concentrations when exposed to acid or alkaline electrolytes, and required calibration with appropriate diluent concentration; however, error in the normal atmospheric concentration level of 20.9% would be small.

In warm weather, due to high ventilation rates, it seems unlikely that oxygen concentrations in poultry houses will decrease much below ambient levels. However, in winter, oxygen levels may fall much below ambient especially if unvented heaters are used. Occupational Health and Safety (OH&S) (2005) reported that the oxygen sensors' output were affected by atmospheric pressure change, but the effects due to slightly lower-than-atmospheric pressure inside negatively-ventilated poultry houses are so small that they can be safely neglected.

### **2.4. MOS sensor for ammonia measurement**

A semiconductor-based sensor was first used by Brattain and Bardeen (1953) for gas concentration measurement. The first commercial MOS sensor was developed by Taguchi (1971).

#### **2.4.1. Working principle**

Reducing gases (such as methane, ethanol, ammonia, hydrogen sulfide, and carbon

monoxide) can increase the conductivities of n-type semiconductors and decrease the conductivities of p-type semiconductors due to the charge transfer reaction between the atmospheric gas and sensing material (Barsan and Weimar, 2003). Change in conductivity is proportional to the gas concentration. To be more specific, a polycrystalline porous layer of the MOS allows gas molecules to diffuse into it. With change in the dominant molecules (oxygen or target gas) the electrical properties of the metal oxide grains are changed, therefore leading to the increase or decrease in the conductivity.

Barsan and Weimar (2001) concluded that different oxygen species were formed and dominated the surface at different temperatures, ranging from molecular-ionic species ( $\leq 150$  °C) to atomic-ionic species at higher temperatures. As the semiconductor heats up, it donates an electron to the oxygen molecule which is transformed into ionic oxygen. This process helps build the acceptor layer for reacting with reducing-type target gases. For n-type MOS, the chemisorption of oxygen on the metal oxide surface requires free electrons from the conduction band and increases the energy band which increases the amount of energy required by the electrons to cross the Schottky barrier between grains (high resistance). This will make n-type MOS a highly resistive surface and p-type a highly conductive surface. In the case of n-type MOS, when the sensor is exposed to reducing gases (e.g., ammonia), the oxygen ions free the electrons. The freed electrons will be released into the conduction band resulting in decrease in the resistance.

Ihokura and Watson (1994) reported that palladium, platinum, or gold could be used as catalysts to improve the MOS sensor's sensitivity and selectivity. Two models have been proposed to explain the mechanism of surface doping: catalytic effect and Fermi energy control. The catalytic effect theory states that the catalyst facilitates the dissociation of certain gases, and therefore, decreases the response time while increasing the sensitivity and selectivity (Fierro, 2006). The Fermi energy theory states that the electronic coupling within the catalyst and semiconductor controls the conductivity, and the catalyst oxidation is dependent on the composition of the sample gas which will help to improve the sensor's performance (Yamazoe, 1991). But these theories have not been validated because recent operando approach used for observing sensor are all far from the true sensing condition.

### **2.4.2. Influencing factors**

The performance of MOS sensor can be degraded by many influencing factors. Several gases, e.g., hydrogen, nitrogen dioxide, hydrogen sulfide, iso-butane, methane, ethanol, carbon monoxide, nitrogen monoxide, and propane can cause cross sensitivity with ammonia MOS sensors (Nanto et al., 1986; Barsan and Weimar, 2001). While some of these gases are normally present in poultry houses in very low concentrations, based on information obtained from the manufacturer of MOS sensors (Figaro, 2012), the concentrations of these gases may not be high enough in poultry houses to affect the MOS sensor's accuracy appreciably.

Water vapor can also change the baseline output of the sensor. Gong et al. (2006) reported that oxygen and water vapor molecules reacted on the sensor's surface, reducing its sensitivity. Wang et al. (2010) reported that chemisorption of oxygen caused by the adsorption of water vapor molecules decreased the sensor's response area, thereby decreasing its sensitivity. Several reaction mechanisms to explain water vapor influence on MOS sensor outputs have been proposed (Heiland and Kohl, 1988; Henrich and Cox, 1994). These mechanisms separately focus on the water vapor reaction with lattice oxygen and adsorbed oxygen; the experimental validation of the mechanisms is beyond the scope of this project.

### **2.4.3. Methods to improve sensor performance**

Advances in fabrication technology for MOS sensors have improved sensitivity and reliability. Santra et al. (2014) reported that their CMOS-based single wall carbon nanotube (SWCNT) sensor for ammonia had excellent response at 200 ppm ammonia at room temperature, cost less than the MOS sensor, and had low variability. Mani and Rayappan (2013) reported that use of spray pyrolysis technique to fabricate MOS ammonia sensor allowed their sensor to measure 25 ppm ammonia with response and recovery times of 20 and 25 s, respectively. These two studies indicated that efforts to develop new fabrication techniques to improve MOS sensor performance and reduce variability are ongoing.

MOS sensors possess inherent variability which causes some difficulties during sensor calibration. Seifert et al. (2009) used the conductance over time profiles (CTPs) method for MOS sensor calibration that required a single point calibration and significantly improved the calibration efficiency and decreased the cost of using MOS sensor. Seifert et al. (2009)

showed use of their method reduced analysis error to <15%.

Using suitable desiccants and sorbents to remove moisture and interfering gases to improve the sensors' selectivity is another option as suggested by Mizsei (1995). This would require taking gas samples and analyzing them on the GC-MS to identify interfering gases and apply appropriate filters. However, because most desiccants sorb ammonia, using desiccants to improve the selectivity of ammonia MOS sensors is a challenge.

There is debate on how water vapor influences sensor output. However, based on empirical evidence, water vapor's influence on the MOS sensor's response can be accounted for by using compensation equations. Sohn et al. (2007) used partial least squares (PLS) method to develop a calibration formula for 12 different Figaro TGS MOS sensors to compensate for moisture's influence that yielded credible and accurate measurements.

## **2.5. Summary of literature review**

In summary, there are many different ammonia and oxygen monitoring methods and each method has its own advantages and disadvantages. In this project, for developing a low-cost, portable ammonia and oxygen monitoring system, based on review of literature, the MOS (ammonia) and EC (oxygen) sensors were considered to be the most appropriate. The performances of both of these types of sensors are affected by other gases as well as relative humidity, temperature, and air speed. The influence of many interfering gases can be neglected due to their low concentrations in the poultry house environment. Where these influences cannot be neglected, as in the case of water vapor, using treatments (e.g., using desiccants, compensation equations, or compensation circuits) could improve the sensors' performances.

### 3. Material and Methods

In this chapter, first the three brands of MOS ammonia sensors were compared. Then the selected ammonia sensor was tested using synthetic gas mixture and later, with air exhausted from a chamber containing poultry litter. Then, the comparison of two brands of oxygen sensors are described. Thereafter, three units of the ammonia – oxygen sensor system were assembled. Finally, the three units were tested.

#### 3.1. Ammonia sensor testing

In this section, first the methodology used to compare the three sensors is described and then the procedure used to test and calibrate the selected sensor is detailed. Based on literature review, three commercially-available MOS ammonia sensors were selected for comparison in this study (Table 3.1). All three sensors have tin oxide semiconductor layers. Detailed information, e.g., accuracy, precision, response time, or standard calibration curve were not available from the manufacturers.

Table 3.1. Make, price, and measurement range of the three MOS ammonia sensors

Model	SP-53B	TGS-2444	MiCS-5914
Make	FIS, Japan	Figaro, Japan	SGX, Switzerland
Price (\$)	33	62	20 <sup>[a]</sup>
Range (ppm)	5-150	10-300	1-500

<sup>[a]</sup>Approximate price that includes a Teflon 0.45-micron filter, 1.5-inch PVC pipe, 1.5-inch PVC cap, and 10-pin surface-mount device (SMD) package.

##### 3.1.1. Comparison of ammonia sensors

To compare the responses of the three ammonia sensors at different ammonia concentrations and RH values, a humidification system was assembled as described below. The data acquisition system is also described. Thereafter, the method for comparing the three ammonia sensors is described.

##### Humidification system

To test the impact of RH on sensor response, first, a one air-steam humidifier (Fig. 3.1)

was assembled and evaluated to obtain RH values in low (40-60%) and high (80-90%) ranges. Lab air (at  $\sim 3$  L/min) was first dried by drawing through a  $3 \text{ \AA}$  molecular sieve scrubber housed in a culture tube. Then this dried air was routed through the humidifier column (also a culture tube) containing tap water (Fig 3.1). The desired RH range of the air mixture entering the testing chamber was achieved by changing the distance  $d$  (distance between the liquid surface and tip of the tube, Fig 3.1). In the test chamber, temperature – RH sensor (Make: Campbell Scientific, US; Model: CS500-L; Accuracy:  $\pm 3\%$  over 10-90% RH at  $20 \text{ }^\circ\text{C}$ ) was used for measuring the RH value of the air mixture.

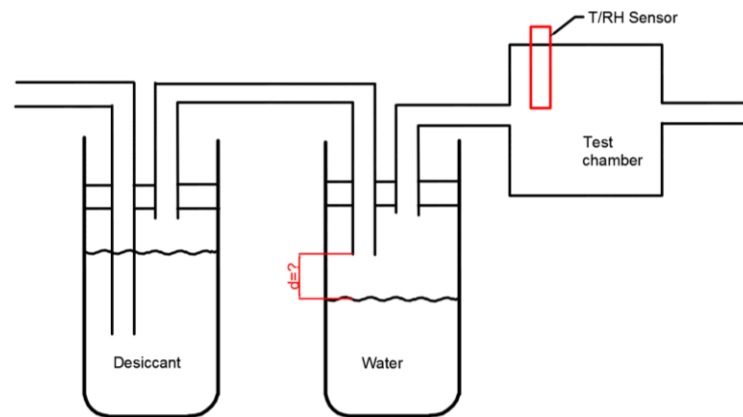


Figure 3.1. One air-stream humidifier set-up. The desiccant used was  $3 \text{ \AA}$  molecular sieve. Tap water was used for humidification.

However, the one air-stream humidifier required constant attention to maintain the distance  $d$  (Fig. 3.1.) for target RH range and it did not provide the high RH values required in this study. So a two air-stream humidifier was designed and used for sensor calibration (Sec. 3.1.2). Lab air was drawn through separate vacuum pumps and the air was released beneath the liquid surface; for high RH requirement, both streams were humidified whereas only one stream was humidified for moderate RH requirement. Then, by adjusting the ratio of these two air-streams using accurate flowmeters with needle valves (Make: DWYER; Model: RMA-21-SSV; Accuracy:  $\pm 5\%$ ), desired RH range in the lab air was obtained.

### Data acquisition system

Raw data from the sensors were collected and stored on a datalogger (Make: Campbell

Scientific, Inc., Logan, UT; Model: CR-1000) (Fig. 3.2). The datalogger measured the MOS sensors' voltage outputs in mV. Since the temperature-RH sensor was also a Campbell Scientific product, the data logger directly displayed RH in percentage, and temperature in Celsius or Fahrenheit. The data logger was programmed for, both scan and store intervals of 5 s.

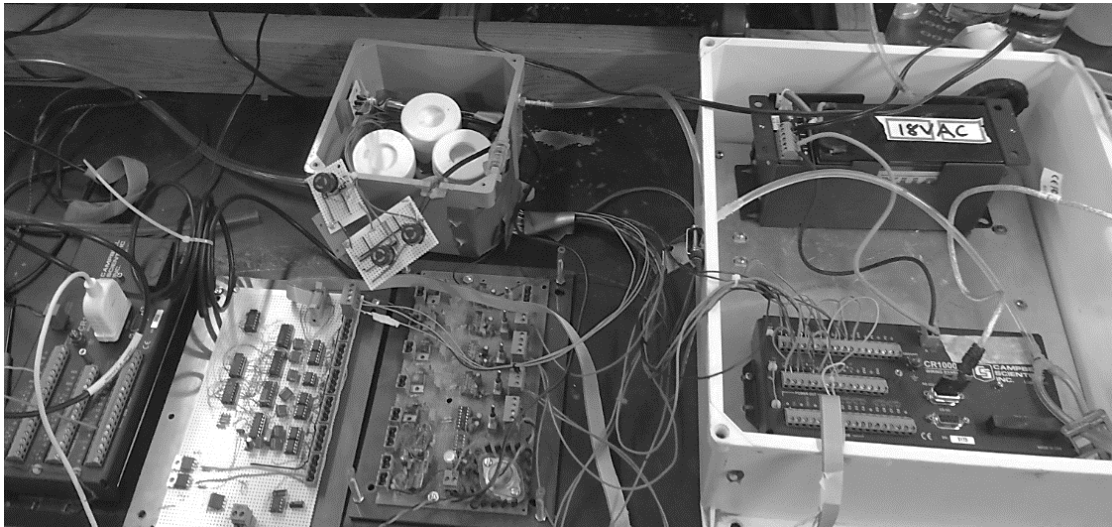


Figure 3.2. Data acquisition system and test chamber for lab testing.

### **Measurement of the variabilities of the temperature and RH sensors**

Temperature sensor (Make: Texas Instruments; Model: LM34DZ; Accuracy:  $\pm 1.7$  °C; Price: \$5 ea.), and RH sensor (Make: Honeywell; Model: HIH-4000-001; Accuracy:  $\pm 3.5\%$ ; Price: ~\$25 ea.) responses were collected and recorded by the datalogger. During the tests, the three sensing systems were tested under the same environment. Therefore, the variabilities of the temperature and RH sensors could be measured.

### **Measurement of sensors' responses**

A multi-point ammonia concentration test was performed for measuring the three sensors' responses to changing ammonia concentrations. By applying the voltage divider design as shown in Figure 3.3, a suitable size of the loading resistor ( $R_L$ ) was evaluated and used for reading the sensor resistance ( $R_S$ ) change in the targeted ammonia concentration range. The loading resistors were 15 k $\Omega$  for MiCS-5914 and 100 k $\Omega$  for both SP-53B and TGS2444.

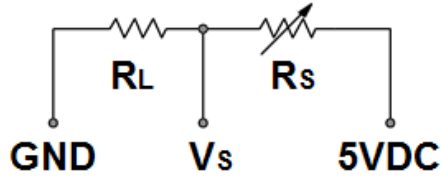


Figure 3.3. Voltage divider circuit design.  $V_S$  is sensor output measured across the loading resistor ( $R_L$ ) and  $R_S$  is the sensor resistor.

In the comparison test, one Figaro TGS2444 sensor (due to its higher price), three FIS SP-53B sensors, and three SGX MiCS-5914 sensors were placed in a 1.5-L PVC test chamber (Fig. 3.4). Following the manufacturer’s guidelines, the SGX MiCS-5914 sensors were placed in individual PVC cells with  $0.45\ \mu\text{m}$  PTFE filters for controlling ammonia diffusion into the cells (Fig. 3.2), while the Figaro TGS2444 sensor and FIS SP-53B sensors were supplied fully-packaged. An external 5VDC power supply were used to power the seven tested sensors.

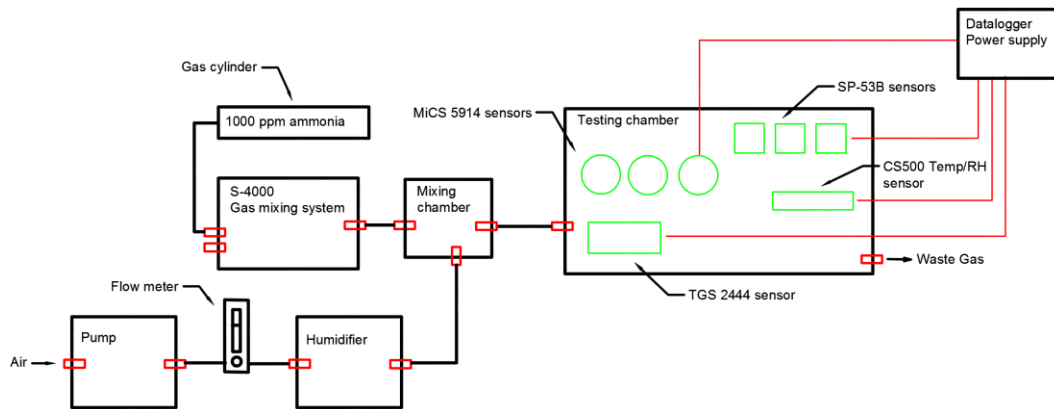


Figure 3.4. Set-up for comparing the three types of ammonia sensors in the lab

A gas mixing system (Make: Environics, Tolland, CT; Model: S-4000) was used to control the flow rate of 1,000-ppm ammonia (balance  $\text{N}_2$ ) from a NIST-certified pressurized cylinder (Supplier: Airgas, Raleigh, NC). The gas mixing system had three mass flow controllers (1-10 mL/min, 50-500 mL/min, 3-30 L/min) with an accuracy of  $\pm 1\%$ . Since MOS sensors require close to ambient oxygen concentrations ( $\sim 21\%$ ) to drive the redox

reaction on the sensor’s surface (Figaro, 2005), lab air supplied by a vacuum pump was blended with ammonia in different proportions to obtain the desired concentration. A flow meter (Make: DWYER; Model: RMA-21-SSV; Accuracy:  $\pm 5\%$ ) was used to control the flow rate of the lab air. The background lab air had  $<50$  ppb ammonia as measured continuously using a CL ammonia analyzer (Make: Thermo Fisher Scientific, Beverly, MA; Range: 0-20 ppm).

Five levels of ammonia concentration (5, 15, 25, 50, and 100 ppm) under low RH (40%) conditions were generated (Table 3.2) to evaluate the response of the MOS sensors. Due to the flow rate limitation of the mass flow controllers of the gas mixing system, total air flow rates varied (Table 3.2). It was assumed that difference in air speeds, due to difference in air flow rates did not affect sensor response. The one-stream humidification system (Fig. 3.1) was used to generate the required RH. A second test using a higher RH of 75% was conducted with three ammonia concentrations (25, 50, and 100 ppm) using the air flow rates shown in Table 3.2 to see if there was ammonia concentration  $\times$  RH interaction based on plot of ammonia concentration vs. mV output at different RH values for each type of sensor. Ammonia concentration  $\times$  RH interaction could not be determined statistically because only one Figaro sensor was used for comparison testing. Each test (concentration - RH combination) lasted for 15 min.

Table 3.2. Flow rates and ammonia concentrations for comparing the three ammonia sensors

Ammonia conc. (ppm)	Ammonia-N <sub>2</sub> mixture flow rate (mL/min)	Lab air flow rate (L/min)	Total airflow rate (L/min)
5	50	8.00	8.050
15	55	3.00	3.055
25	90	3.00	3.090
50	180	3.00	3.180
100	360	3.00	3.360

All the sensors were new and were heated for 48 h prior to the test following the manufacturers’ recommendations. The tests were conducted at room temperature (26.4 –

29.0 °C). As will be discussed in Chapter 4 (Results and Discussion), the Figaro TGS2444 sensor performed better than the other two sensors. So, two more TGS2444 sensors were purchased, and each TGS2444 sensor was calibrated individually, as discussed below. Because MOS sensors require periodic purging and the sensors were not purged in this test, data collected in this test were not used for sensor calibration.

### **3.1.2. Ammonia sensor calibration**

#### **Moisture influence on sensor response**

Two options to reduce the influence of moisture on the Figaro TGS2444 sensor were examined. First, the possibility of using a calcium oxide (CaO) filter to absorb moisture was examined. Being a basic desiccant, CaO will not adsorb ammonia gas whereas all other desiccants that are not strongly basic will adsorb ammonia in addition to absorbing moisture. However, use of CaO desiccant to completely dry the air stream was discarded due to its slow moisture removal rate. Another option was to formulate moisture compensation equations based on the sensors' outputs to different combinations of RH and ammonia concentrations; this was the approach that was used and is described in Chapter 4.

#### **Calibration set-up**

During calibration, the accuracy of the sample gas mixture concentration is crucial. Lab air flow rate, set at 10 L/min was measured and controlled with a high accuracy flowmeter (Make: OMEGA; Model: FLDA3422G; Accuracy:  $\pm 2\%$ ). As in the previous testing, 1,000 ppm ammonia (balance N<sub>2</sub>) flow rate was controlled by the gas mixing system; by varying the flow-rate of 1,000 ppm ammonia cylinder, four ammonia concentrations were achieved (Table 3.3).

Table 3.3. Flow rates and ammonia concentrations for sensor calibration

Target ammonia conc. (ppm)	Ammonia-N <sub>2</sub> mixture flow rate (mL/min)	Lab air flow rate (L/min)	Calculated ammonia conc. (ppm)
5	50	10	4.98
15	152	10	14.97
25	256	10	24.96
50	500	10	47.62

To ensure accuracy of the sample gas concentration, the flowmeter air flow rate was verified by the S-4000 gas mixing system before every test. Additionally, 2% boric acid scrubbers (150 mL) were used to determine the time-weighted concentration for every concentration level. Time averaged ammonia-N concentration measured by an acid scrubber was calculated as eq. [3.1] (Shah et al., 2013).

$$C_G = \frac{C_L * V}{Q * \Delta t} \quad [3.1]$$

In eq. [3.1],  $C_G$  is the time averaged ammonia –N concentration in the sample gas ( $\text{mg m}^{-3}$ ),  $C_L$  is ammonium-N concentration in scrubber solution which was determined by colorimetry ( $\text{mg m}^{-3}$ ),  $V$  is the volume of the scrubber solution ( $\text{m}^3$ ),  $Q$  is the air flow rate through the scrubber ( $\text{m}^3 \text{min}^{-1}$ ) and  $\Delta t$  is the duration of the measurement (min).

### Calibration chamber and experiment set-up

In the test performed to compare the three types of sensors (Sec. 3.1.1), a ~1.5 L PVC chamber was used. But in this large chamber, it took 3-5 min to achieve the required ammonia concentration which was longer than the response time of the TGS2444 sensor. Hence, three individual 325 mL chambers made of ~0.15 m long 2 in. PVC pipes and with tight-fitting end caps were assembled. These chambers had barbed hose connections at both ends for air movement.

In each chamber, a TGS2444 ammonia sensor mounted on a Figaro evaluation module (EM2444), a temperature sensor, and an RH sensor were placed close together. Compared with the method used for comparison of the three ammonia sensor brands described earlier, an important modification in this calibration exercise was the use of EM2444 evaluation module for the TGS2444 sensor. For optimal sensor performance, for a 250 ms cycle, the

EM2444 applies a heating voltage of 4.8 V for the first 14 ms followed by 0 V for the rest of the cycle (Figaro, 2012). For the same cycle, circuit voltage of 0 V is applied by the EM2444 for the first 2 ms, 5 V for the next 5 ms, and 0 V for the remainder of the period. Detection is done 7 ms into the cycle (Figaro, 2012). Circuit voltage pulsing at the right time and duration in the cycle can reduce the potential long term resistance drifts caused by the migration from heater material to the sensing element material under high temperature and RH condition (Figaro, 2012). Compared to the evaluation module built in the BAE Dept., the EM2444 was more compact and performed better.

To ensure that all chambers received the same air flow rate ( $\sim 2.5$  L/min), air flow into each chamber was controlled with a flowmeter with valve (Make: GILMONT; Model: GF-8321-1401; Accuracy:  $\pm 5\%$ ). Excess air was bypassed into a filter packed with 3 Å molecular sieve to remove the ammonia prior to being discharged into the lab. Calibration was done at room temperature ( $\sim 25$  °C). The two desired RH levels (55% and 80%) were obtained by blending, in different proportions, two lab airstreams (Fig. 3.5).

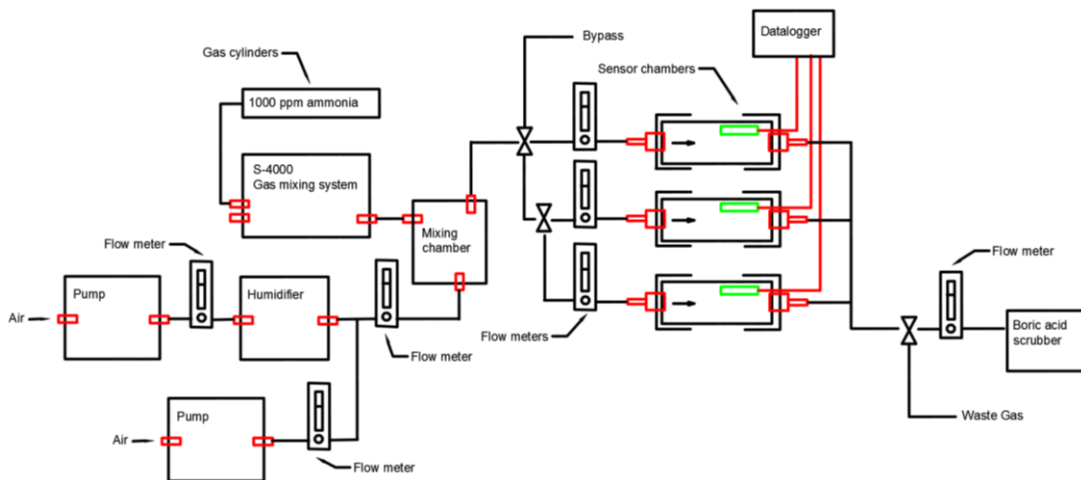


Figure 3.5. Set-up for calibrating the three TGS2444 sensors.

As shown in Figure 3.5, a portion of the gas mixture exhausted from the chambers was routed through a 2% boric acid scrubber (150 mL) to determine time-averaged ammonia concentration. Since the flow rate into the scrubber was measured and controlled with a

flowmeter with valve (Make: Cole-Parmer; Model: EW-32461-50; Accuracy:  $\pm 3\%$ ), ammonia concentration in the air stream could be calculated using eq. [3.1]. The rest of the ammonia-laden exhaust was again scrubbed through a 3 Å molecular sieve filter before being released into the lab.

### **Air flow rate impact on sensor response**

To evaluate the impact of flowrate on sensor response, one TGS2444 sensor was tested at four different air flow rates (1, 2, 3, and 5 L/min) at a concentration of 25 ppm using the set-up used for the sensor calibration. Air flow into the chamber was controlled with a flowmeter with a control valve (Make: Cole-Parmer; Model: EW-32461-50; Range: 0.4 to 5 L/min; Accuracy:  $\pm 3\%$ ) and the excess air was scrubbed through a 3 Å molecular sieve filter before being released.

### **Hysteresis testing**

One TGS2444 sensor was tested for 45 min with alternating 25 and 50 ppm ammonia sample mixture with 3 min exposure time for each concentration to determine if there was any hysteresis. Purging the sensor with filtered clean air between measurements will be needed if hysteresis is observed.

### **Short-term drift testing**

For determining the short-term drift, one TGS2444 sensor was exposed to 25 ppm ammonia continuously for 80 min at fixed RH and temperature. The sensor's short-term drift test was performed to decide how long measurements could be taken before the sensor required purging.

#### **3.1.3. Sensor testing with poultry litter chamber exhaust**

In this test, the TGS2444 sensors (and their RH and temperature compensation equations) were evaluated for their abilities to measure ammonia concentration in air exhausted from a chamber with poultry litter. Poultry litter was obtained from the NCSU Broiler Unit and placed in a ~10 L PVC chamber with a porous base (Fig. 3.6) to allow lab air (<50 ppb ammonia) to be pulled through the poultry litter using a vacuum pump.



Figure 3.6. Porous base of the poultry litter chamber.

Refrigerated poultry litter (2-3 L) was placed in the chamber with a perforated base (Fig. 3.6) and its temperature was allowed to equilibrate to room temperature ( $\sim 25$  °C) before starting the study. Lab air pulled through the bottom of the chamber was humidified by a water bath beneath the litter (Fig. 3.7). Measurements with the Drager Pac III meter with an XS NH<sub>3</sub> electrochemical sensor (Make: Drager Safety; Range: 0 to 300 ppm) indicated that the ammonia concentration in the air exiting the chamber was  $>300$  ppm, beyond the upper limit of measurement of the Drager sensor. Therefore, a second vacuum pump was used to pull in lab air ( $<50$  ppb ammonia) and the two air streams were blended using accurate individual flowmeters equipped with sensitive control valves to obtain the target range of ammonia concentrations (10-20, 30-40, or 40-50 ppm). Thirteen 10-min tests were conducted, with the first eight events conducted around 25 °C. The last five tests were conducted to test the sensor at low ammonia concentrations ( $<20$  ppm); room temperature due to the changed setting of the room air conditioner was around 20 °C.

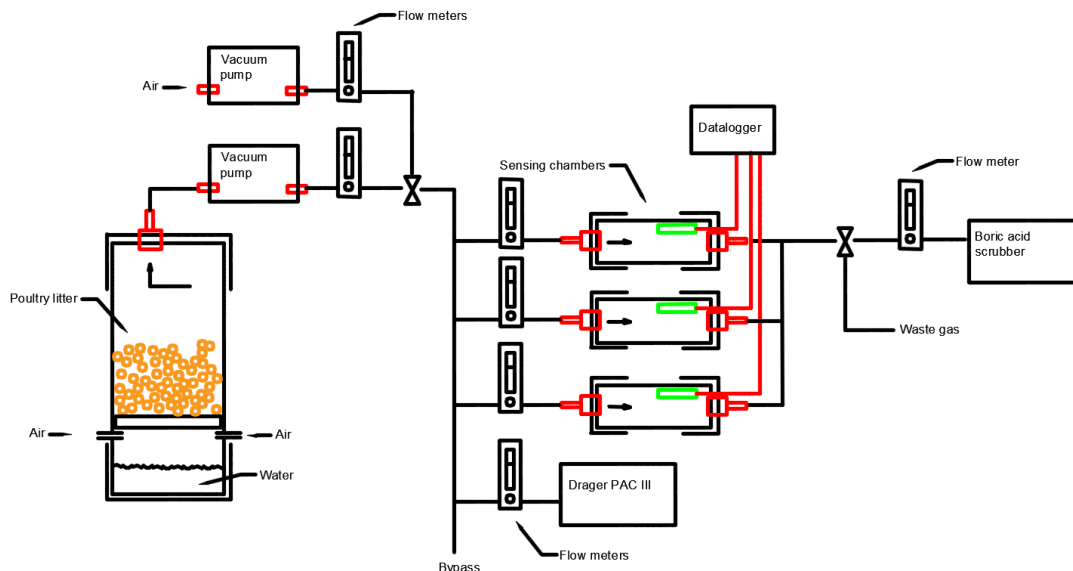


Figure 3.7. Chamber testing set-up using poultry litter as the ammonia source.

The target ammonia concentration in the blended air (confirmed with the Drager electrochemical sensor) was divided into three equal air streams using individual flowmeters with control valves and routed into the sensing chamber (same as Sec. 3.1.2). As in Sec. 3.1.2, each sensing chamber had an ammonia sensor, temperature sensor, and RH sensor. Data from these sensors were recorded every 5 s by the data acquisition system (Sec. 3.1.1).

The Drager electrochemical sensor was also used to monitor real-time ammonia concentrations during the experiment while a 2% boric acid scrubber (Fig. 3.7) was used to determine the 10-min time-weighted average ammonia concentration. The exhaust air bypassing the scrubber and exiting the Drager sensor was treated in a molecular sieve filter prior to release. To prevent degradation of the Drager electrochemical sensor due to long-duration exposure to ammonia, the electrochemical sensor was purged with lab air for 15-min after each test. A three-way solenoid pinch valve (Make: Cole-Parmer, Vernon Hills, IL) controlled by time delay relay (Make: Dayton Electric Manufacturing Co., Lake Forest, IL; Model: 6A855) was used to set the time periods for purging and sampling of the Drager sensor. The testing was performed at room temperature ( $\sim 25$  °C) and lab air was not humidified.

### 3.2. Oxygen sensor testing

Based on literature review, two oxygen sensors, namely, KE-25 (Make: Figaro, Japan; Range: 0-100%; Accuracy:  $\pm 1\%$  (full scale); Response time:  $14 \pm 2$  s; Price \$79), and SGX-40X (Make: SGX, Switzerland; Range: 0-25%; Price: \$38) were selected for comparison. Both of these oxygen sensors provide current outputs, so amplifier electrical circuits were applied to convert current to voltage outputs. The oxygen sensors' voltage outputs were collected and processed by the same data acquisition system described in Sec. 3.1.1. The experimental set-up for comparing the two oxygen sensors is shown in Figure 3.8.

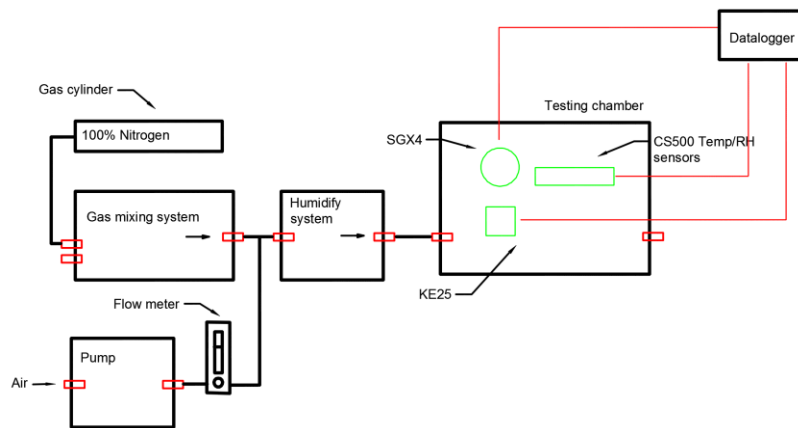


Figure 3.8. Layout of the oxygen sensor testing system.

Three oxygen concentrations (17%, 19%, and 21%) were prepared by mixing air streams (Table 3.4) from NIST-certified 100%  $N_2$  (controlled by gas mixing system) and lab air (controlled by flow-meter) (Figure 3.8). It was assumed that the lab air had an oxygen concentration of 20.9%.

Table 3.4. Flow rates and oxygen concentrations used for oxygen sensor comparison

Oxygen conc. (%)	Lab air flow rate (L/min)	$N_2$ flow rate (L/min)	Total flow rate (L/min)
17	1.7	0.4	2.1
19	1.9	0.2	2.1
20.9	3	0	3

Since it was more important to track changes in oxygen concentrations rather than measure them with great accuracy, based on an ambient oxygen concentration of 20.95% (OSHA, 2005), it was assumed that the lab air had a slightly lower concentration. Because oxygen solubility in water is very low, the air stream was directly routed through the humidification system. Testing was done under both low (10-20%) and high (80-90%) RH conditions (measured by CS500 temp/RH sensor) to test for the influence of RH on sensor performance. Due to the relatively high cost of these sensors, only one unit of each type was tested.

### **3.3. Sensor system fabrication**

#### **3.3.1. Data acquisition, control, and display**

In order to develop a hand-held ammonia-oxygen sensing system, a data processing system comprised of an Arduino Mega microcontroller (Make: SainSmart, Lenexa, KS), an 81.3-mm (3.2-in.) thin-film transistor (TFT) touch screen (Make: SainSmart, Lenexa, KS) were assembled. The microcontroller obtained raw data from the ammonia, oxygen, RH, and temperature sensors, processed the data into useful information and displayed it on the screen. Whereas the touchscreen can also be used to control the sensing system, in this study, for simplicity, it was solely used for display.

#### **3.3.2. System assembly**

The system lay out is shown in Figure 3.9 and the assembled unit is shown in Figure 3.10, in a 203 mm ×127 mm ×76 mm plastic enclosure with a lid. The total mass of the system is less than 1.4 kg (3 lb), and the total cost of the components is <\$450 (Table 3.5). The life times for the ammonia and oxygen sensors as reported by manufacturer exceeds 1 yr (Figaro, 2012). In addition to ammonia and oxygen concentrations, the system also measures and displays temperature and RH.

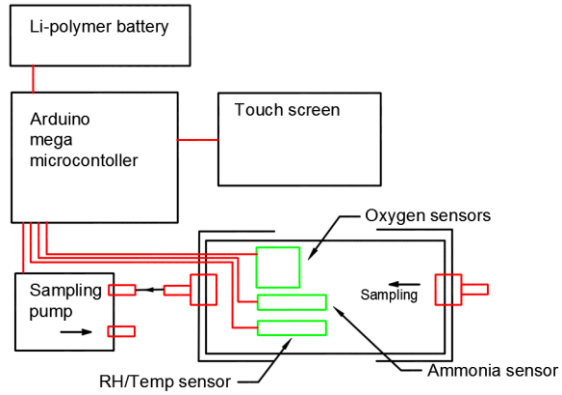


Figure 3.9. Lay out of the ammonia - oxygen sensor system

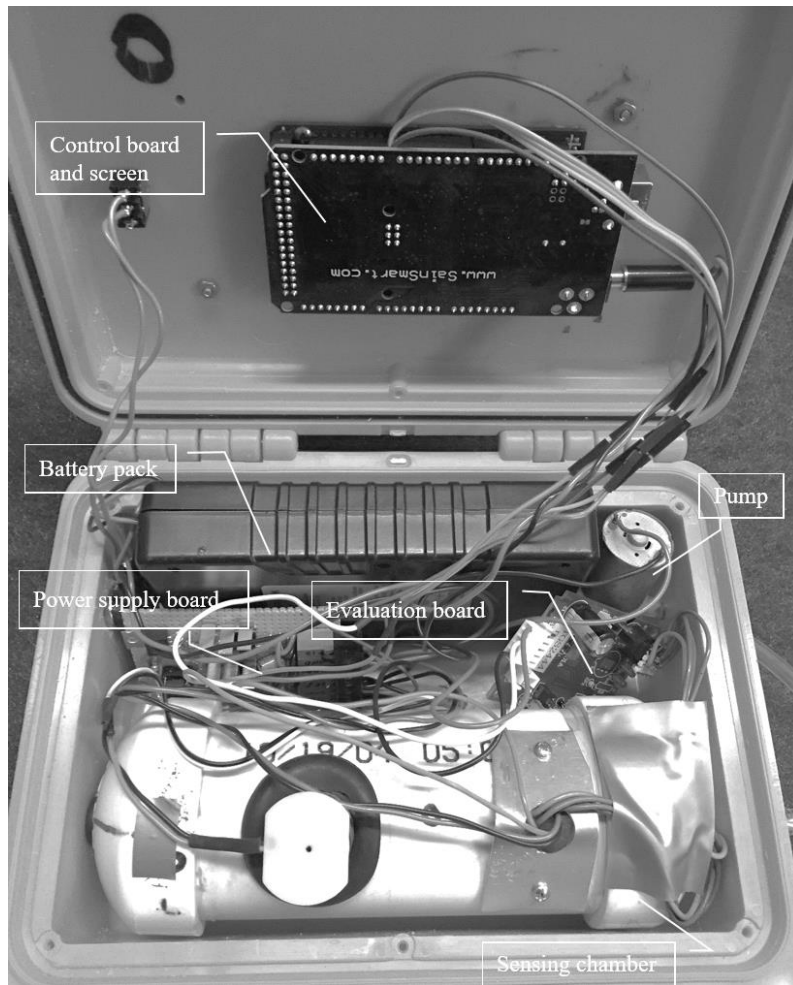


Figure 3.10. Picture of the assembled sensor system

Table 3.5. List of components used in the ammonia – oxygen sensor system and their prices (including shipping and handling). Prices do not include taxes.

<b>Item</b>	<b>Vendor</b>	<b>Description</b>	<b>Price</b>	<b>Qty</b>	<b>Subtotal</b>
TGS2444 sensor	Figaro	Ammonia sensor	\$62	1	\$62
EM2444 module	Figaro	Evaluation board	\$104	1	\$104
KE-25 sensor	Figaro	Oxygen sensor	\$79	1	\$79
HH-4000-003 sensor	Honeywell	RH sensor	\$25	1	\$25
LM34DZ sensor	TI	Temperature sensor	\$5	1	\$5
Arduino Mega	SainSmart	Microcontroller	\$30	1	\$30
Touch Screen	SainSmart	3.2-in. Touch Screen/Shield	\$30	1	\$30
Battery Pack	Talentcell	Rechargeable 12V 6000 mAh Li-ion battery	\$30	1	\$30
Vacuum Pump	OME	2.5L/min micro pump	\$20	1	\$20
PVC pipe	LOWES	Sch. 40 2 in. PVC pipe (0.15 m length)	\$0.38	1	\$0.38
PVC Cap	LOWES	Sch. 40 2 in. PVC cap	\$0.71	2	\$1.42
Miscellaneous connectors		Connectors, tubing, etc.	\$5	-	\$5
Plastic enclosure	Serpac	8”×5”×3”enclosure	\$33	1	\$33
<b>Total</b>					<b>\$424.8</b>

### 3.3.3. Power supply

The total current demand of the display screen, microcontroller, pump system, and sensors was ~600 mA. Therefore, a rechargeable 12VDC Li-ion battery pack, namely, the Talentcell 12VDC battery pack (Capacity: 6000 mAh) was selected as the power supply for this system. This battery has a built-in protection circuit, and slow charging function (10 h for full charge) to prolong battery life. It was estimated that the sensor system could continuously operate for 8 h on a full charge.

### **3.4. Fabricated units testing**

Three fully fabricated units (namely, UNIT1, UNIT2, and UNIT3) were tested using air exhausted from a chamber containing poultry litter (same as sec. 3.1.3) at two temperature levels (20 and 30 °C), and two ammonia concentration levels (10-25 and 35-50 ppm). An attempt to test the system at 30 °C and 80% RH was abandoned due to the inability of the humidification system to raise the RH to that high level at 30 °C. In any case, the utility of the RH compensation equation had been validated earlier.

The ammonia – oxygen sensor system was compared with the ammonia gas tube (Make: RAE Systems, Sunnyvale, CA; Normal range: 1-30 ppm; Extended range: 2-72 ppm; Accuracy: 15-20% for >50 ppm, 10-12% for ≤50 ppm) and Drager Pac III meter with an XS NH<sub>3</sub> electrochemical sensor to assess how this experimental unit compared with devices commonly used for ammonia management in poultry houses. An Isotemp-220 digital control water bath (Make: Fisher Scientific; Range: 0 to 100 °C) was used to heat the air mixture for testing at the higher temperature. The air mixture was routed through 61 m of vinyl tubing in 65 °C water to obtain the desired temperature. The layout for this test is shown in Figure 3.11. The poultry litter gas sampling and the method used to concentration the control was described in section 3.1.4.

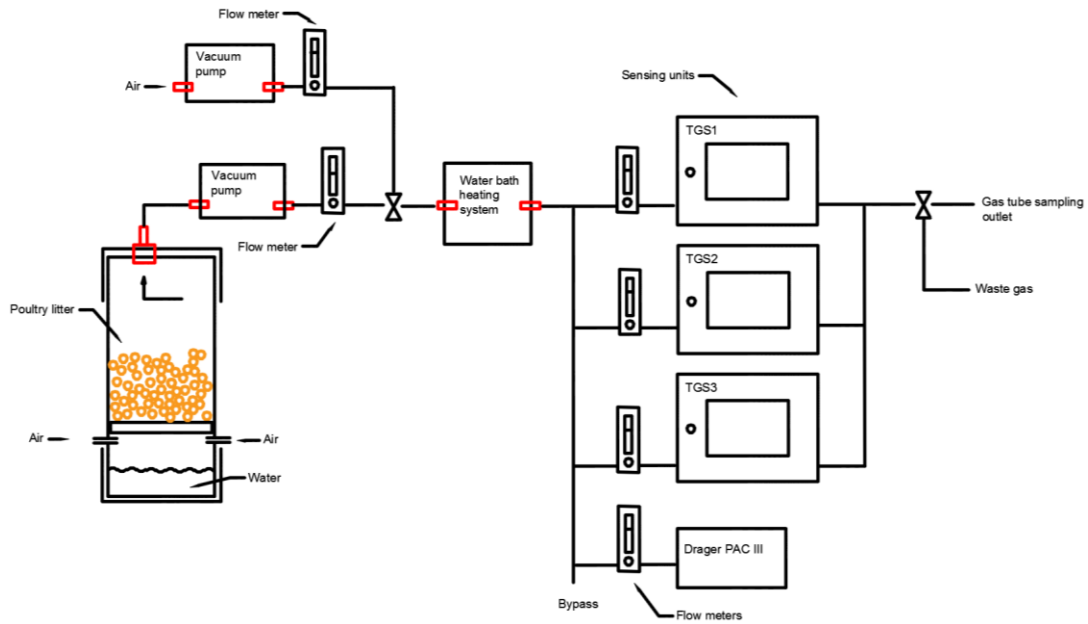


Figure 3.11. Layout of the system used to test the fabricated units.

Ideally, use of the water bath should have allowed heated ammonia laden air to be transferred simultaneously to all the sensor units arranged in parallel. But due to heat loss between the water bath and the sensor units, it was not possible to increase air mixture temperature from room temperature (20 °C) to the target temperature of 30 °C for all three units simultaneously. Therefore, the system was simplified as shown in Figure 3.12, and only one unit was compared at a time with the Drager EC analyzer and gas tube at five ammonia concentration levels (range: 5-72 ppm). Tubing length between the water bath to the unit was kept as short as possible to reduce heat loss. A total of 10 L/min of ammonia laden air was heated in the water bath with only 2 L/min used for sensor testing; the remaining 8 L/min was scrubbed in the molecular sieve scrubber and released.

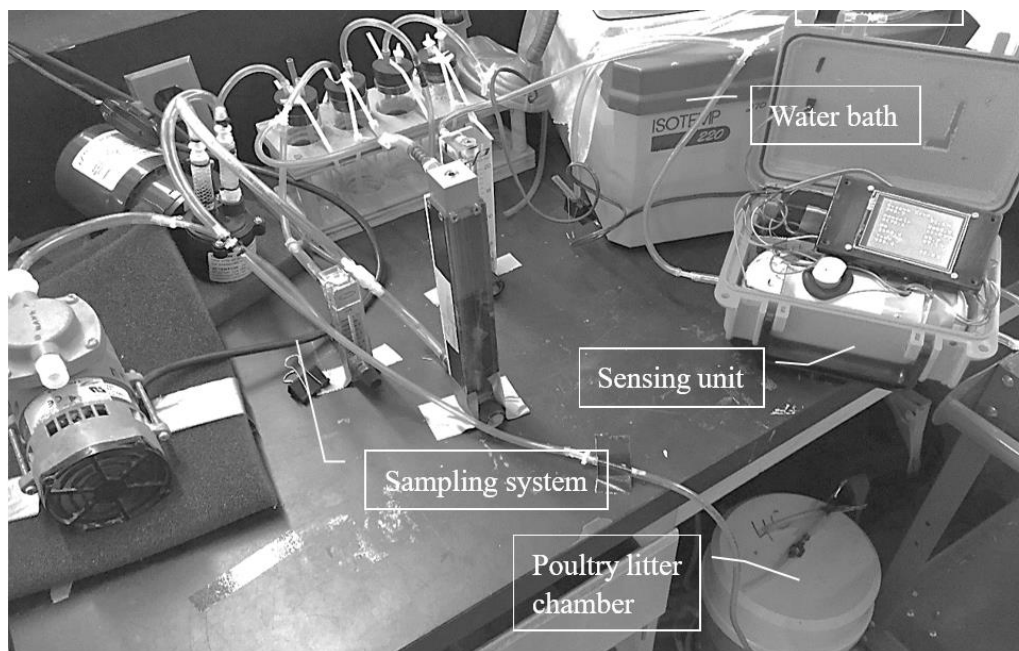


Figure 3.12. Picture of the modified fabricated units testing system for high temperature test.

During fabrication, the RH sensor in UNIT3 were damaged. The RH sensor in UNIT1 under-measured RH at high RH (discussed later) which led to underestimation of ammonia concentration at high RH compared with the other two units. Therefore, these two defective RH sensors were replaced prior to testing of the completed units. The new RH sensors in UNIT1 and UNIT3 were evaluated using the RH compensation equation for UNIT2. Finally, three completed units were tested outdoors to evaluate responses of oxygen sensors to ambient oxygen concentrations.

### 3.5. Ancillary considerations

Apart from the design issues discussed above, some precautions were taken during the unit's fabrication and operation. The presence of silicone vapor could irreversibly damage the MOS sensor (Figaro, 2012). Similarly, PVC cements containing volatile organic compounds (VOCs) affect the MOS sensor (Figaro, 2012). Therefore, all silicone- and VOC-based sealants and adhesives were excluded; so Teflon tape was used for sealing.

A filter is required to protect the sensors from particulate matter (PM) present in the air. Therefore, a hydrophobic filter was installed to exclude PM, as shown in Figure 3.13. The

hydrophobic polyurethane foam filter would prevent, moisture absorption and hence, might also reduce ammonia. No tests were performed to study ammonia sorption by the filter, but given the filter's coarse nature and 5 ppm detection limitation of the device, the filter would likely not affect sensor performance.

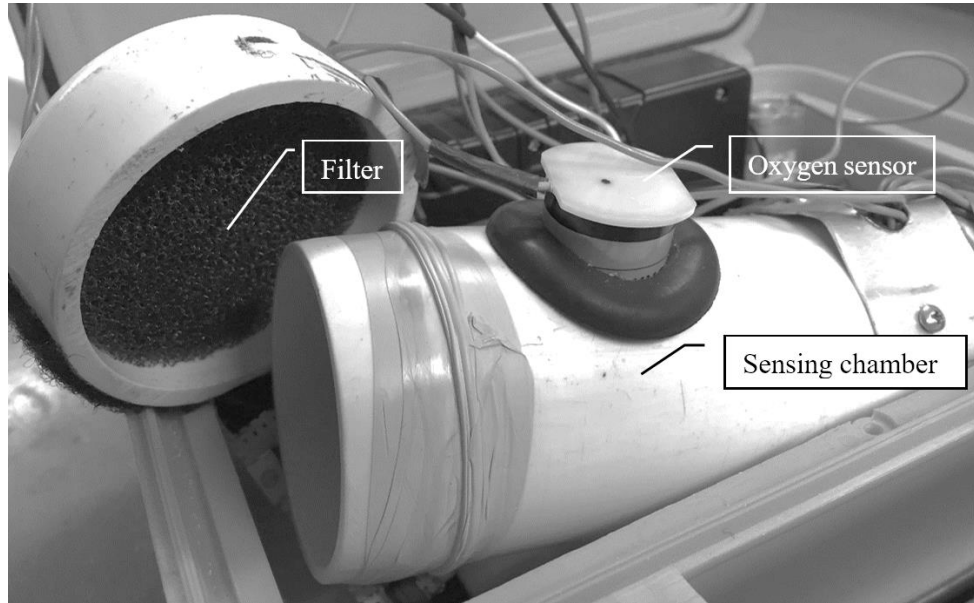


Figure 3.13. Picture of hydrophobic filter installed in the sensor chamber

Biosecurity is a major concern when moving the sensor system from one farm to the next. Currently, the disease of concern is avian influenza (AI). While AI can be inactivated rapidly at 37 °C, under dry conditions, AI can be inactivated in a few minutes even at 25 °C (Chumpolbanchorn et al., 2006; Association of Avian Veterinarians, 2006). However, no testing to determine AI inactivation was performed in this study.

## 4. Results and discussion

In this chapter, the results of comparison of the three ammonia sensors are presented. Then, the results of testing of the ammonia sensor under various conditions are discussed. The results of the comparison of the two oxygen sensors are presented. Finally, the results of testing of the assembled sensor system are presented.

### 4.1. Ammonia sensor testing

#### 4.1.1. Comparison of ammonia sensors

In the lab, when the three MOS ammonia sensors were evaluated at ~40% RH, the Figaro TGS2444 sensor responded more rapidly to changes in ammonia concentrations, yielding clearer step functions than the FIS SP-53B and the SGX MiCS 5914 sensors (Fig. 4.1). Very importantly, while the Figaro sensor has a published sensitivity of 10 ppm, it clearly responded to 5 ppm, the minimum detection limit desired for this sensor system.

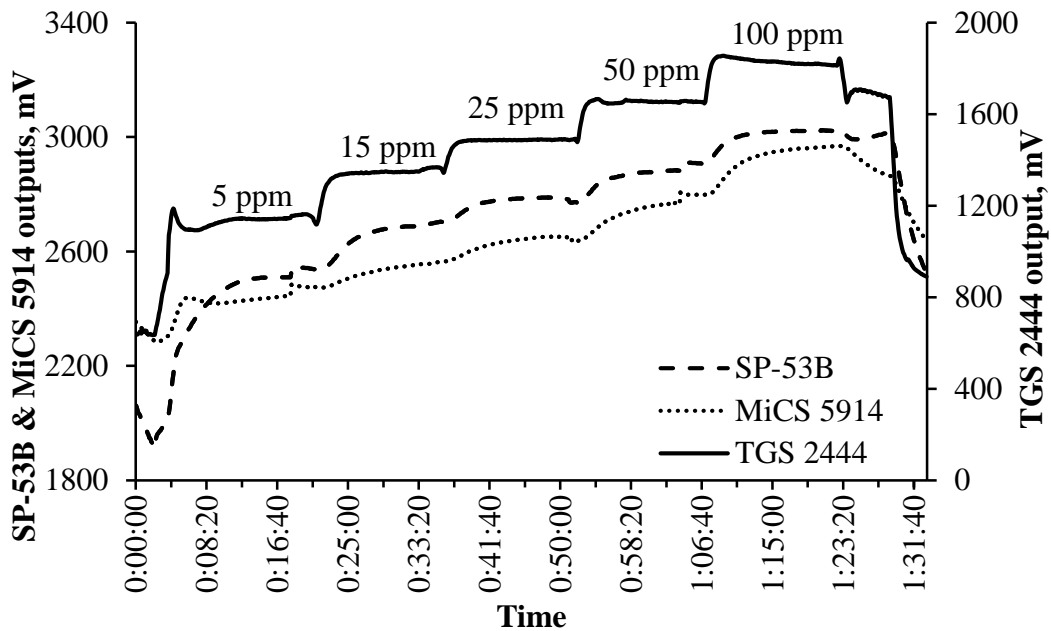


Figure 4.1. Analog outputs of the three MOS ammonia sensors at 26 °C to 29 °C and 43% RH to 35% RH. Each trend line is the output of a single sensor. The three sensors are: FIS SP-53B, SGX MiCS 5914, and Figaro TGS2444. For each sensor, readings were scanned and recorded every 5 s.

The three ammonia sensors were tested at several ammonia concentrations at two RH levels (40% and 75%). The Figaro sensor's response to different ammonia concentrations at the low and high RH paralleled one-another (Fig. 4.2), better than the responses of the FIS (Fig. 4.3) or SGX (Fig. 4.4) sensors. This indicated that the Figaro sensor's response to change in RH seemed to be less affected by the ammonia concentration than the two other sensors. Further, the bigger difference in mV output at two RH values for the same gas concentration allowed for better resolution of gas concentration as a function of RH in the Figaro sensor than the two other sensors. So developing a compensation equation to account for the effect of RH on the Figaro sensor would be simpler and more accurate than developing correction equations for the other two sensors. Hence, despite the Figaro sensor being the most expensive of the three different makes of sensors, it was selected for use in the ammonia – oxygen sensor system.

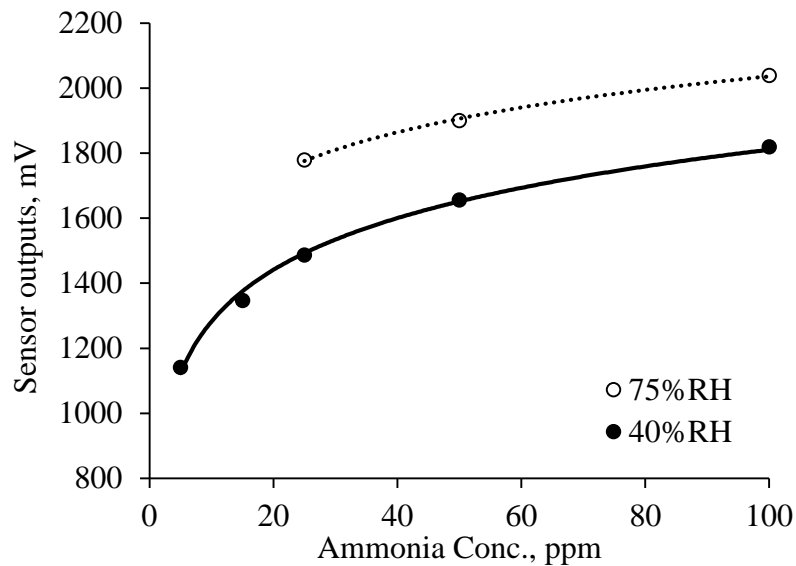


Figure 4.2. Response of a single Figaro TGS2444 sensor to changes in ammonia concentrations and RH conditions. The sensor was not tested at high RH at 5 and 15 ppm ammonia concentrations. Each data point is an average of five readings.

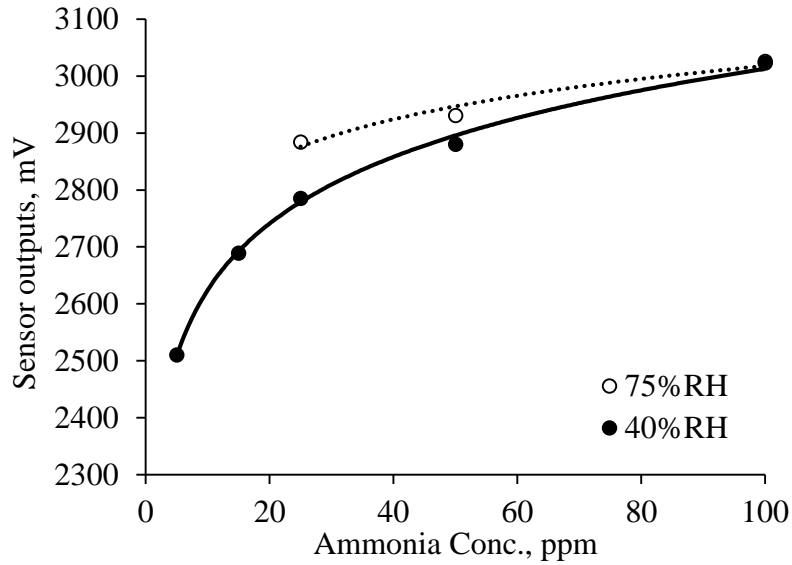


Figure 4.3. Response of a single FIS SP-53B sensor to changes in ammonia concentrations and RH conditions. The sensor was not tested at high RH at 5 and 15 ppm ammonia concentrations. Each data point is an average of five readings.

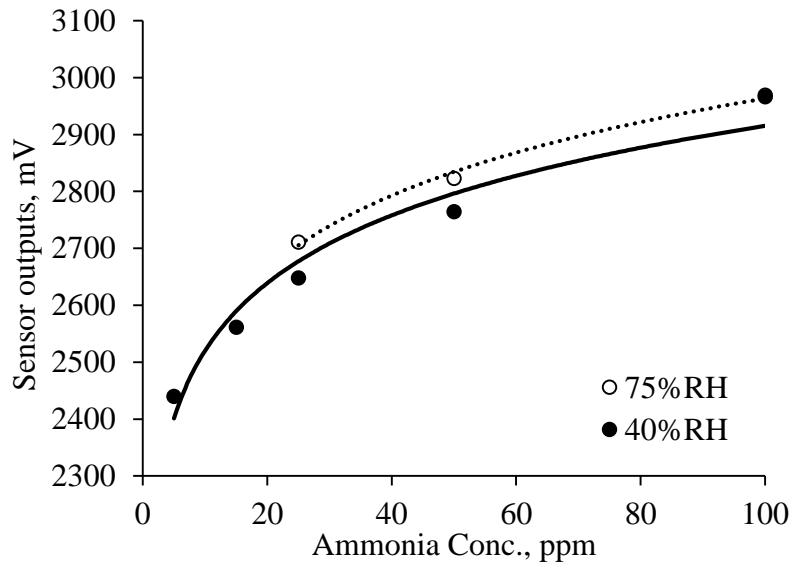


Figure 4.4. Response of a single SGX MiCS 5914 sensor to changes in ammonia concentrations and RH conditions. The sensor was not tested at high RH at 5 and 15 ppm ammonia concentrations. Each data point is an average of five readings.

#### 4.1.2. Ammonia sensor calibration

Ammonia sensor calibration required completion of several other tests. They are: evaluation of the two-stream humidifier, airflow rate impact on sensor response, sensor response as affected by purging (hysteresis), short-term drift testing, and testing of temperature and RH sensors. Since these tests provided the basis or the information to calibrate the ammonia sensors, the results of these tests precede the results of ammonia sensor calibration.

##### Two air-stream humidifier

An effective humidifier was needed to calibrate the ammonia sensors at different RH values. As mentioned in Chapter 3, the one-stream humidifier required constant attention and did not produce the high RH values required for testing and calibration. Hence, the two-stream humidifier was tested. As the proportion of the humidified air-stream increased, RH of the sample air increased linearly and with a very high  $r^2$  value (Fig. 4.5).

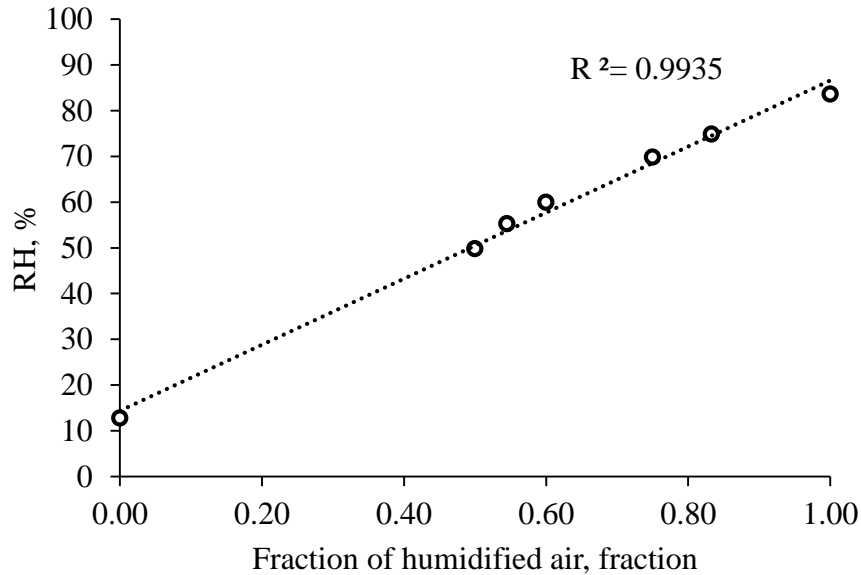


Figure 4.5. Relationship between chamber RH and fraction of humidified air in the two air-stream humidifier as measured with the CS 500 temperature/RH sensor. Each data point is an average of five readings.

The two-stream humidifier yielded relatively stable chamber RH values by changing the proportion of dried (~13% RH) and humidified air-stream flow rates in the lab at around ~25 °C (Fig. 4.6). However, the desired RH range can only be maintained if the lab temperature does not change. Further, the required water level had to be maintained by adding water. The average RH drift for the two air-stream system was 2.9%/h which is lower than the accuracy of the RH sensor ( $\pm 3.5\%$ ). Hence, adding water hourly to maintain the water level would be acceptable.

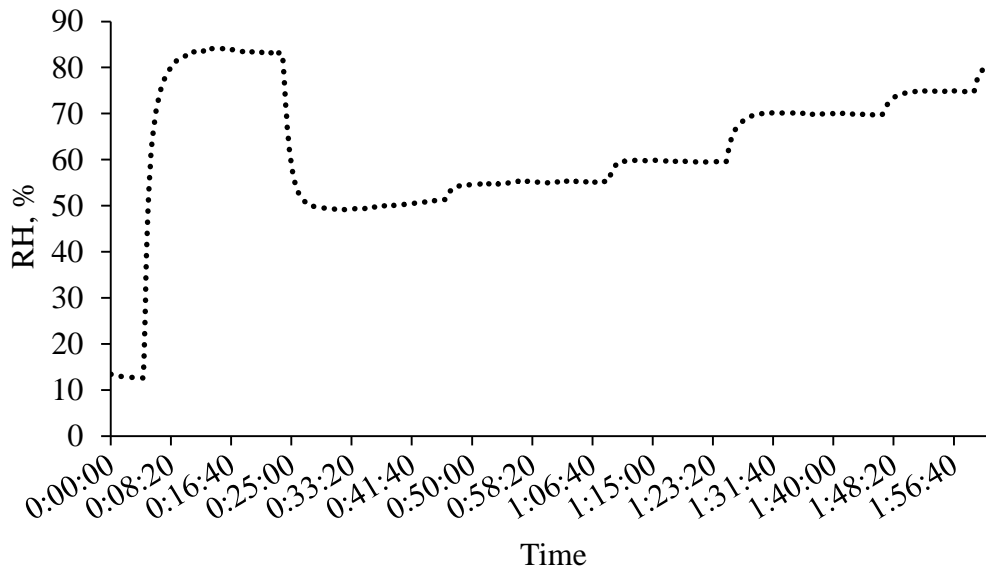


Figure 4.6. Change in test chamber RH for different proportions of the humidified and dry air-stream. Total airflow rate was 4-6 L/min and the testing was performed in a temperature range of 24.6 °C to 25.1 °C with a room RH of 55%. Readings were taken every 5 s.

### Chamber airflow rate impact on sensor response

In an aspirated sensor system design, sensor response can be affected by the air speed that the sensor ‘sees’. Therefore, testing was performed to assess the response of the ammonia sensor to different airflow rates. One TGS2444 sensor was tested under fixed 25 ppm ammonia concentration at four levels of airflow rate (1, 2, 3, and 5 L/min). Sensor output increased with the flow rate (Fig. 4.7). The TGS24444 sensor system read 3082 mV at 1

L/min, 3163 mV at 3 L/min, and 3203 mV at 5 L/min. The difference in the sensor's reading between 1 and 5 L/min was 121 mV. Hence, the response of the TGS2444 sensor is flow-dependent in the range of 1 to 5 L/min.

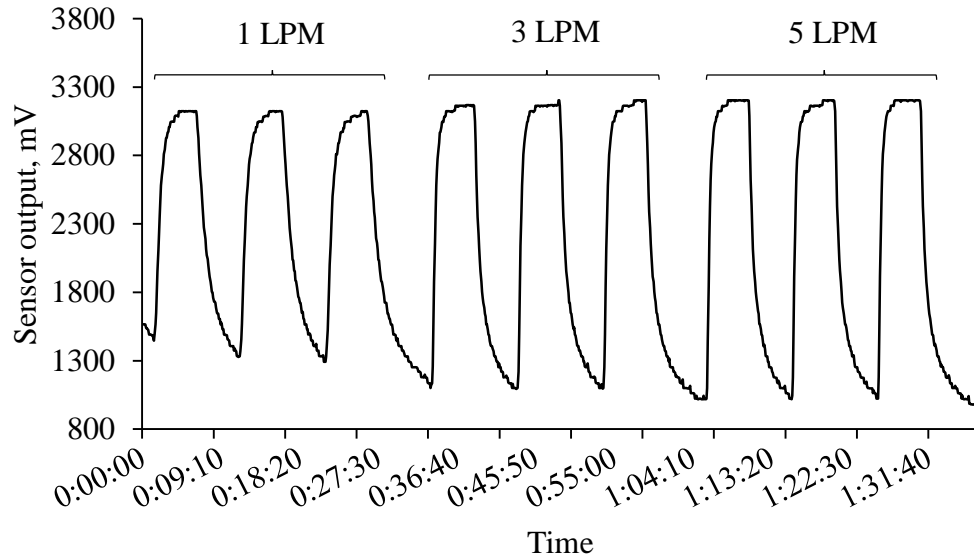


Figure 4.7. Response of a single TGS2444 sensor to 25 ppm ammonia concentration at three airflow rates (1, 3, and 5 L/min). The sampling and purging time was 5 min. This study was conducted at a temperature of 25 °C and 61% RH. Readings were taken every 5 s.

As exhibited in Fig. 4.8, the same sensor unit was tested with airflow rates of 1, 2, and 3 L/min. At 2 and 3 L/min, the sensors outputs were 3167 and 3162 mV, respectively, but at 1 L/min it was 3095 mV. Hence, the sensor's response was barely affected in the airflow rate range of 2 to 3 L/min. Given that the sensor response was affected very little in the 2-3 L/min range, calibration performed in this airflow rate range was considered valid.

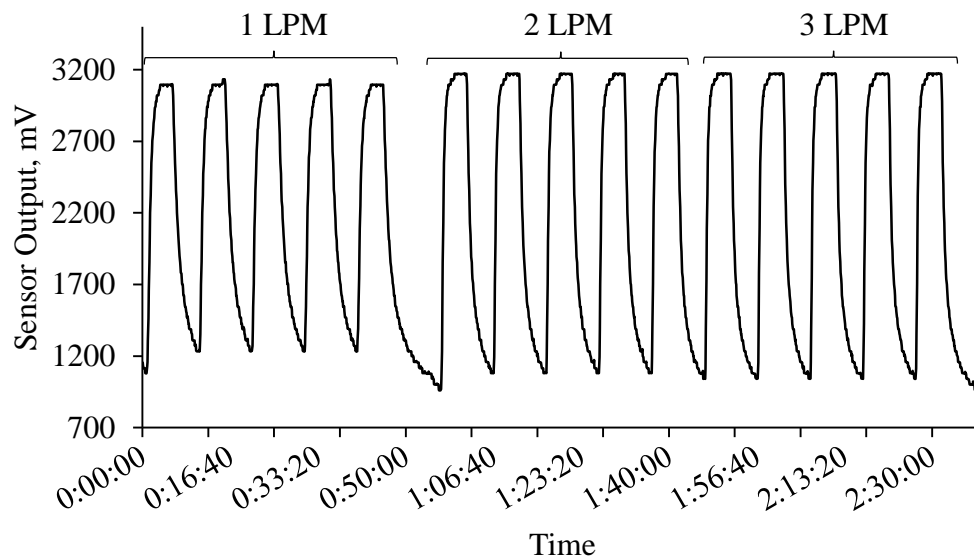


Figure 4.8. Response of a single TGS2444 sensor to 25 ppm ammonia concentration at three airflow rates (1, 2, and 3 L/min). The sampling and purging time was 5 min. This study was conducted at a temperature of 26 °C and 59% RH. Readings were taken every 5 s.

#### **Impact of changing concentrations on sensor response**

One unit of TGS2444 sensor was tested with alternating 25 and 50 ppm ammonia concentrations with 3 min of exposure at each concentration. Sensor response was very rapid, remained quite stable over the 46-min run, and did not display any hysteresis (Fig. 4.9), i.e., the sensor response seemed to be unaffected by whether gas concentration was on the increase or decrease. The response time for the sensor was ~60 s from low to high concentration, and ~75 s from high to low concentration because it took longer to flush out the high concentration ammonia gas mixture from the chamber.

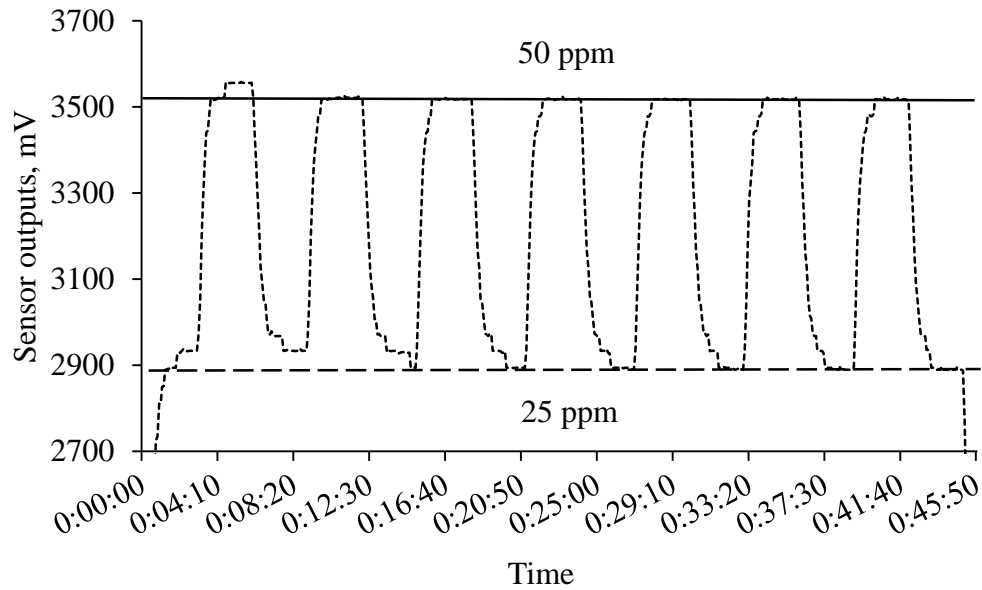


Figure 4.9. Response of a single TGS2444 sensor to alternating 25 and 50 ppm ammonia concentration with 3 min of exposure at each concentration (fixed RH of ~62% and temperature of 22 °C). Readings were taken every 5 s.

### Short-term drift testing

A test was conducted to measure the short-term drift of the TGS2444 sensor system for 80 min. The test was conducted at fixed lab RH and temperature with continuous exposure to 25 ppm ammonia. As shown in Fig. 4.10, drift was -27.8 mV/h. Very importantly, the low R-square (0.68, Fig. 4.10) indicated that the sensor was relatively unaffected by the duration of continuous operation. The reason for the two dips observed during the test (Fig. 4.10) is unclear. However, the flat response during the last 35-40 mins in this test (Fig. 4.10) and given the small drift and stable response with changing ammonia concentrations (Fig. 4.9), it would be acceptable to take continuous readings for perhaps, up to 40 min in a poultry house, without purging. However, purging the ammonia sensor with ambient air for 2-3 min between poultry houses is still recommended to increase the accuracy and life of the sensor system.

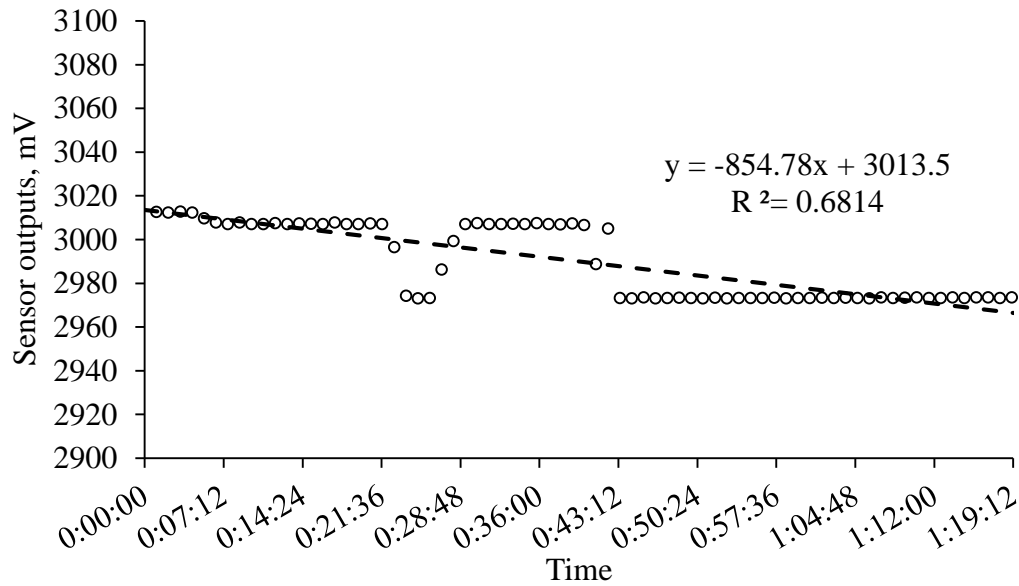


Figure 4.10. Short-term drift of a single TGS2444 ammonia sensor at nominal ammonia concentration of 25 ppm (fixed RH of ~62% and temperature of 22 °C). Each data point is a measurement taken at 5-s intervals.

### Testing variabilities among the temperature and RH sensors

Three low-cost temperature sensors and RH sensors were installed alongside the ammonia sensors as the sensor packages for generating RH/temperature compensation equations, and the variabilities among these temperature and RH sensors were verified during the test. The LM34 temperature sensor provides a voltage output that can be divided by 10 to obtain temperature in Fahrenheit and costs only \$5. When the three LM34 temperature sensors (TEMP1, TEMP2, TEMP3) acquired for use with the TGS2444 sensors were compared in the lab, they displayed considerable variability (Fig. 4.11). Among the three temperature sensors, TEMP1 readings were the closest (<0.5 °C) to the datalogger panel temperature readings and thus could have been the most accurate. TEMP2 and TEMP3 had higher average temperatures than TEMP1 by 5.9 F (3.3 °C) and 1.6 F (0.9 °C), respectively. So, while the difference in temperatures between TEMP1 and TEMP3 was within the accuracy ( $\pm 1.7$  °C) of the LM34 sensor, TEMP2 had unacceptably high temperature readings. However, the outputs of the three LM34 sensors paralleled each other (Fig. 4.11). Therefore,

assuming that TEMP1 was the most accurate, the intercept of TEMP1 was also applied to equations of TEMP2 and TEMP3. The normalized outputs of the three sensors are given in Fig. 4.12. Using a more-expensive temperature sensor would have reduced the uncertainty but would have made the sensor system less-affordable.

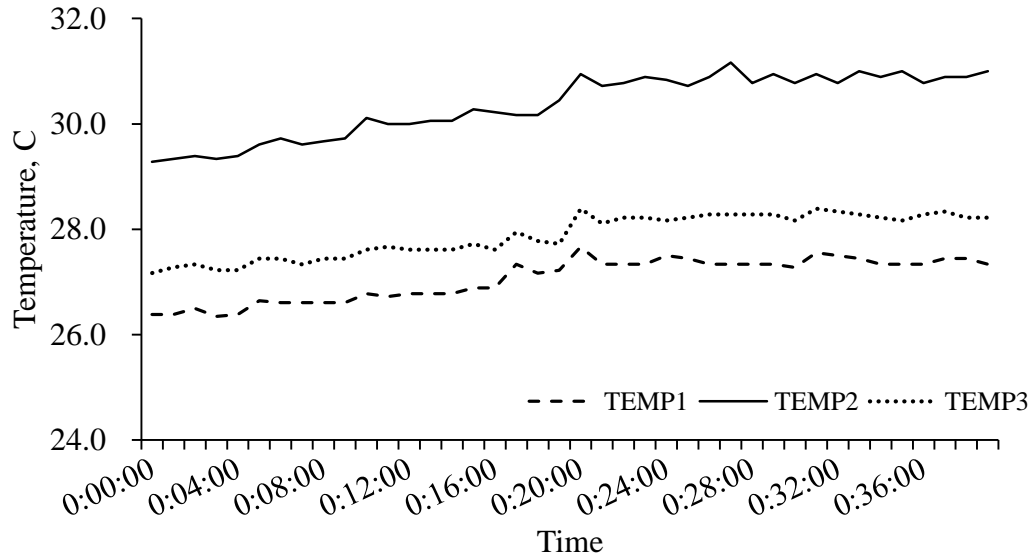


Figure 4.11. Comparison of the three LM34 temperature sensors in the lab. Temperature readings were taken every 5 s.

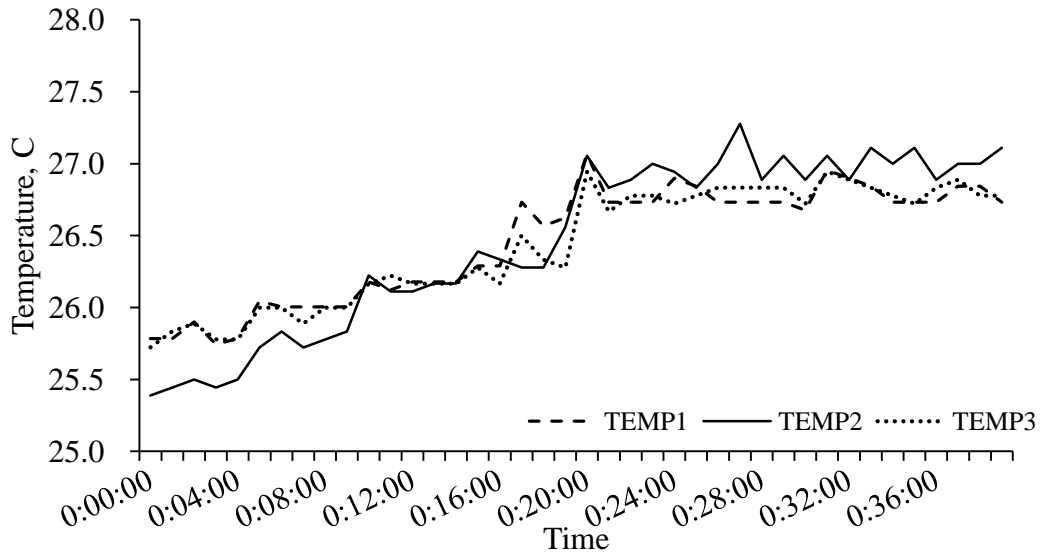


Figure 4.12. Adjusted LM34 temperature sensors outputs.

Three HIH-4000-003 RH (RH1, RH2, RH3) sensors were compared in the lab at  $\sim 25\text{ }^{\circ}\text{C}$ . Percent RH for each sensor was calculated (Fig. 4.13) using the standard calibration curve provided by the manufacturer. Whereas RH2 and RH3 showed good agreement (generally within  $\pm 3.5\%$ , accuracy of the sensor) with one-another, RH1 only showed good agreement with RH2 and RH3 under room RH conditions ( $\sim 55\%$ ) (Fig. 4.13). Under high RH conditions, the RH1 output RH values that were  $\sim 18\%$  lower than the outputs of RH2 and RH3 ( $\sim 80\%$ ) (Fig. 4.13). Since RH measurements during this test were not made using a ‘standard’ RH sensor, it could not be stated with certainty that RH1 under-measured RH. However, in the high RH test, since the air stream was humidified (but not in the low RH test), it could be reasonably assumed that RH2 and RH3, which had similar outputs were more accurate. It would reasonably follow that RH1 displayed greater variability from the mean of the three RH sensors in the high RH range than the other two sensors. As will be discussed later, use of the RH1 sensor affected the output of the ammonia sensor, requiring its replacement.

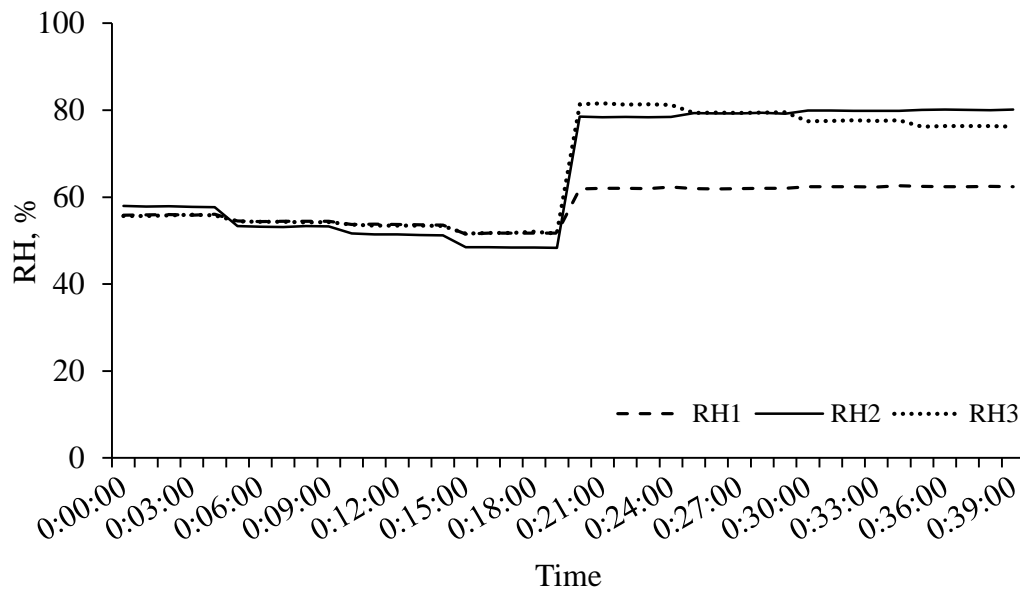


Figure 4.13. Comparison of three HIH-4000-003 RH sensors in the lab. Readings were taken every 5 s.

Variability among the RH and temperature sensors were likely due to use of relatively inexpensive and light sensors to keep the material price of the sensor system below \$500 and its mass less than 1.4 kg (3 lb). More-expensive RH and temperature sensors might have reduced the variability which would be more important for a research-grade instrument, rather than a management-grade instrument which is the focus of this project.

### Testing of variability among the TGS2444 ammonia sensors

Three TGS2444 sensors (namely, MOS1, MOS2, and MOS3) were tested under four ammonia concentration (5, 15, 25, and 50 ppm) under two RH ranges (50-60% and 70-80%) (Fig. 4.14). The sensors' outputs tracked one-another quite closely though MOS2 seemed to give lower outputs than the other two sensors (Fig. 4.14). The TGS2444 sensors responded rapidly to changes in ammonia concentration. (Fig. 4.14).

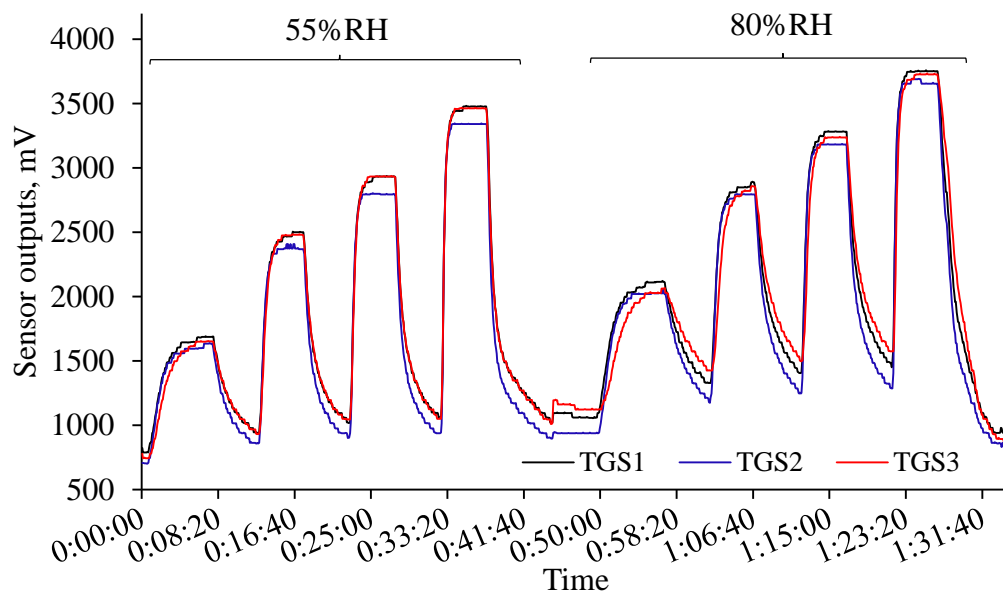
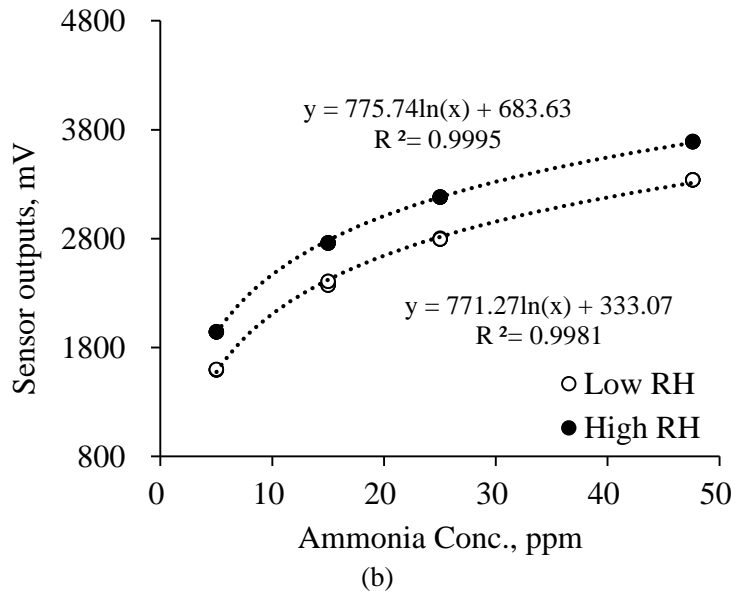
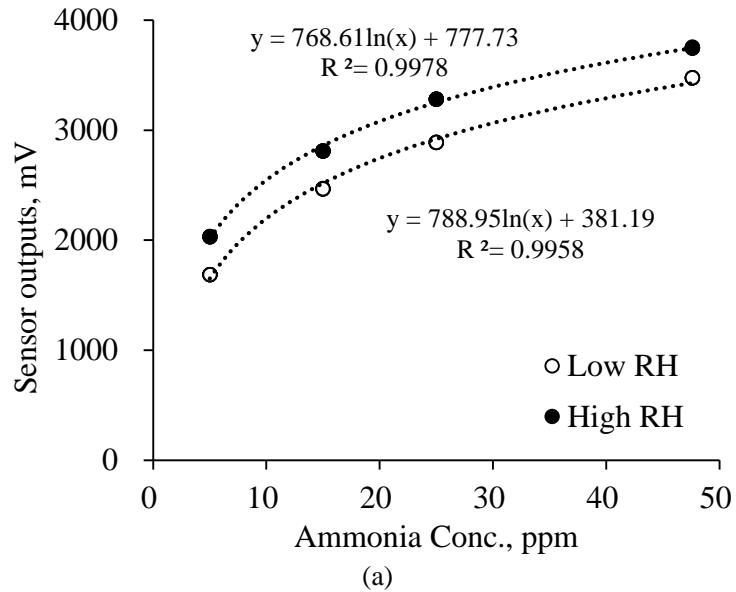


Figure 4.14. Responses of three Figaro TGS2444 sensors to changing ammonia concentrations (5-50 ppm) under low (55%) and high (80%) RH conditions. Measurements were taken every 5 s. Test temperature was ~25 °C.

As shown in Figure 4.15, at fixed RH and temperature, the mV outputs of the three TGS2444 sensors increased logarithmically as ammonia concentration increased from 5 to 50

ppm. More interestingly, each sensor's outputs paralleled one-another at both RH levels which indicated a lack of ammonia concentration  $\times$  RH interaction. In the case of each sensor, the slopes at 55% and 80% RH were similar (Fig. 4.15). However, the slopes and intercepts of the three sensors showed variability among one-another (Fig. 4.15) which might be due to the inherent variability among the sensors (Figaro, 2012).



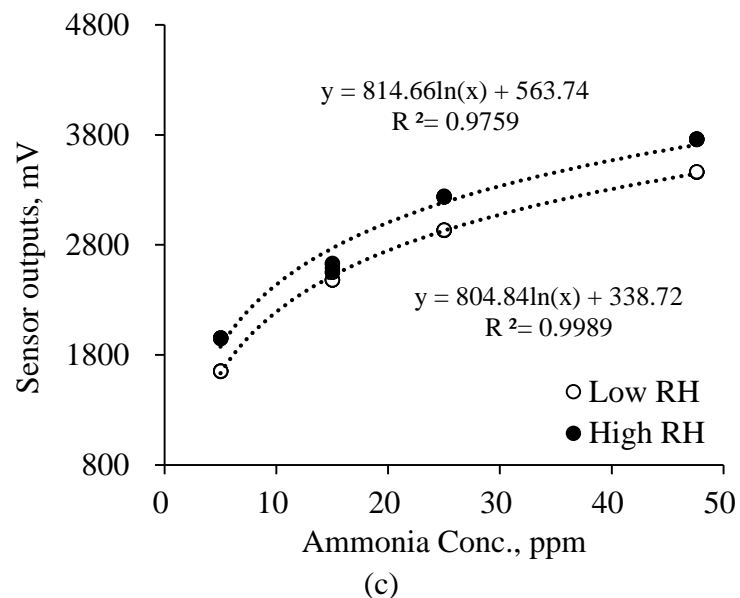


Figure 4.15. Responses of (a) MOS1, (b) MOS2, and (c) MOS3 sensors to ammonia concentrations (5-50 ppm) at low and high RH conditions. Each data point is the average of five readings. Test temperature was ~25 °C.

The mean output of three sensors as a function of ammonia concentration and RH is shown in Figure 4.16. Of the eight data points, only one data point (15 ppm at 55% RH) exhibited relatively high SD (100 mV), probably due to random error; the other data points had low SD, ranging from 32 to 63 mV (Fig. 4.16).

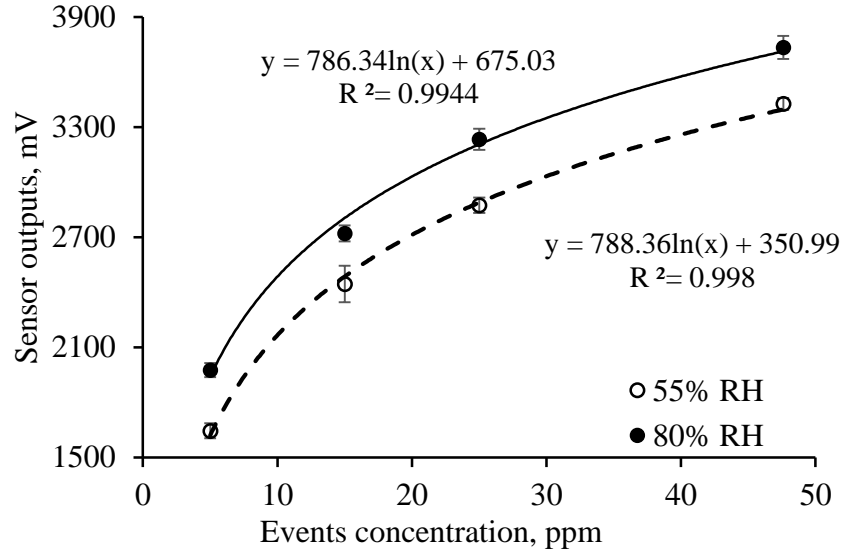


Figure 4.16. Mean of MOS1, MOS2, and MOS3 sensor outputs as a function of ammonia concentration and RH at 25 °C. Each data point is the average of the mean of the three sensors presented in Fig. 4.15 and the error bars are SD values.

### Temperature and RH compensation equations for the ammonia sensors

Based on the temperature and RH data collected, sensor compensation equations were generated. Because the TGS2444 sensor's response is temperature dependent, the sensor's resistance at the test temperature was standardized at 25 °C, the calibration temperature, using eq.[4.1] (Figaro, 2012).

$$R_{Temp} = [1 - C(Temp - 25)] * R_{25} \quad [4.1]$$

In eq. [4.1],  $R_{Temp}$  is the sensor's resistance at test temperature,  $R_{25}$  is the sensor's resistance at 25 °C. Temp is the test temperature (°C), and C is the temperature-dependent coefficient provided by manufacturer. In this study, C (0.01) is the decrease in sensitivity per 1 °C increase within an operating temperature range of 20 to 50 °C (Figaro, 2012).

The sensor's mV output at the test temperature was standardized to calculate mV output at 25 °C using eq.[4.2] and eq. [4.3] (Figaro, 2012; Figaro, 2006).

$$R_{Temp} = \frac{(V_{in} - V_{Temp}) * R_L}{V_{Temp}} \quad [4.2]$$

In eq. [4.2],  $V_{Temp}$  is ammonia sensor mV output at the test temperature;  $V_{in}$  is input voltage (5 VDC).  $R_L$  (10 K $\Omega$ ) is loading resistor in the voltage divider (Fig. 3.3).

$$V_{out} = \frac{V_{in}}{\left(\frac{V_{in}}{V_{Temp}} - 1\right) / [1 - C(Temp - 25)] + 1} \quad [4.3]$$

In eq. [4.3],  $V_{out}$  is standardized ammonia sensor mV output at 25 °C.

The following sensor equations (eq. [4.4] through [4.6]) were generated using SAS (SAS, 2012) based on standardized ammonia sensor mV output (eq. [4.1]) and standardized RH data at 25 °C using multiple linear regression (Ott et al., 2001). It is absolute humidity (g-H<sub>2</sub>O/m<sup>3</sup>) that impacts ammonia sensor response, but compared with RH sensors, absolute humidity sensors are not as widely used and are more expensive. An alternative way for calculating absolute humidity is converting RH at operation temperature to RH at calibration temperature (25 °C) using Magnus-Tetens approximation equation (Heldman and Moraru, 2003). This allowed for calculation of sensor response as a function of humidity ratio.

$$[NH_3]_1 = \exp\left(\frac{V_{out1} - 37.3 * RH_1 + 1703}{813}\right) \quad [4.4]$$

$$[NH_3]_2 = \exp\left(\frac{V_{out2} - 12.9 * RH_2 + 419}{794}\right) \quad [4.5]$$

$$[NH_3]_3 = \exp\left(\frac{V_{out3} - 9.7 * RH_3 + 268}{830}\right) \quad [4.6]$$

In equations [4.4] through [4.6], the subscripts 1, 2, and 3 are values associated with MOS1 (or RH1), MOS2 (or RH2), and MOS3 (or RH3), respectively;  $[NH_3]$  is ammonia concentration (ppm);  $V_{out}$  is standardized (at 25 °C) ammonia sensor mV output; and RH is the standardized RH value at 25 °C. Probably due to manufacturing defects, the coefficient and intercept of the RH1 sensor were substantially greater (eq. [4.4]) than the other sensors. Therefore, in calculating a single equation (hereafter, referred to as the unified equation) for the ammonia sensor (eq. [4.7]), only datasets from MOS2 and MOS3 sensor packages were considered.

$$[NH_3]_{Uni} = \exp\left(\frac{V_{out} - 11.5 * RH + 353.8}{812.4}\right) \quad [4.7]$$

In equation [4.7], the subscripts Uni means the unified equation for TGS2444 sensor package.

### 4.1.3. Poultry litter chamber testing of ammonia sensor

When exposed to ammonia-laden air exhausted from a chamber containing poultry litter, the three MOS sensors had similar responses over the entire duration (Fig. 4.17). However, MOS1 seemed to have consistently lower outputs than the other two sensors which had similar outputs. Results presented in Figure 4.17 were based on application of the equations [4.4], [4.5], and [4.6] to MOS1, MOS2, and MOS3, respectively. Based on the responses of the ammonia MOS sensors, it seemed as if the other gases released by poultry litter, e.g., H<sub>2</sub>, CO, methane, iso-butane, ethanol, nitrogen monoxide, nitrogen dioxide, hydrogen sulfide, and propane (Barsan and Weimer, 2001) might not have been present in the air from the poultry house chamber in sufficient concentrations to affect sensor performance.

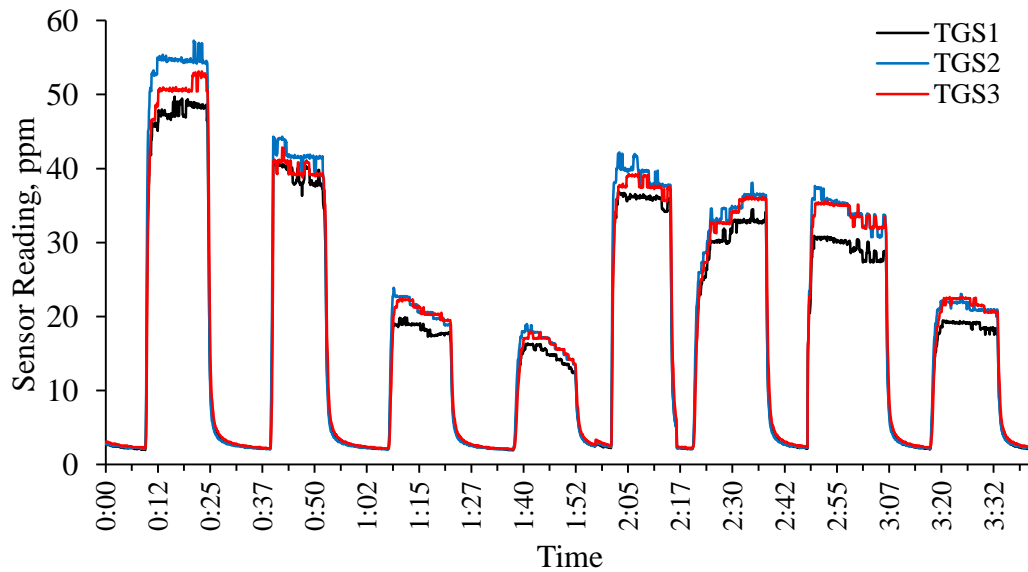


Figure 4.17. Comparison of the outputs of the three ammonia sensors for a wide range of ammonia concentrations over 4 h. Measurements were made every 5 s. Test conditions were 53% RH and 26 °C.

Data presented in Fig. 4.17 represented eight events, each lasting 10 min. For those eight events (1-8), ammonia concentrations measured with the TGS2444 sensors, real-time concentrations measured with a recently-calibrated Drager EC sensor and time-weighted average concentrations measured with boric acid scrubbers are compared in Figure 4.18.

Results for another five events (9-13) were based on tests done on a different date for low concentration (<20 ppm).

Average ammonia concentrations measured with the three MOS sensors based on their individual equations (eq. [4.4]-[4.6]) and unified equation (eq. [4.7]) are compared with the scrubber and EC measurements in Figure 4.18. Difference in ammonia concentrations based on the average of the three MOS sensors (MOS\_AVG, Fig. 4.18) and the unified equation (MOS\_UNI, Fig. 4.18) were quite similar for the individual events (their quantitative differences will be discussed later). In fact, averaged over the 13 events, mean MOS\_AVG and mean MOS\_UNI were equal to one-another (Fig. 4.18). Hence, even the unified equation (eq. [4.7]) worked quite satisfactorily.

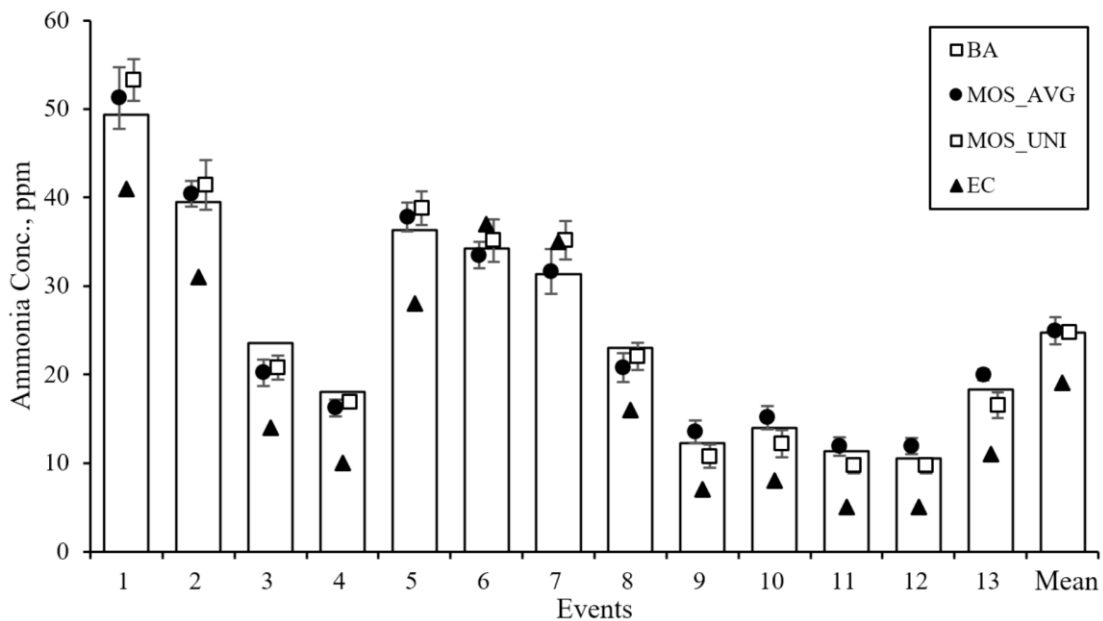


Figure 4.18. Comparison of ammonia concentrations measured with boric acid (BA) scrubbers, Drager EC sensor, and MOS sensors (MOS\_AVG, MOS\_UNI) in air exhausted from a chamber containing poultry litter. MOS\_AVG is the average ammonia concentration of the three MOS sensors based on their individual equation (eq. [4.4]-[4.6]). MOS\_UNI is the average ammonia concentration of the three MOS sensors using the unified equation eq. [4.7]. The dashes indicate SD associated with MOS\_UNI and MOS\_AVG. For each event,

average reading for each MOS sensor is based on 120 readings. The first 8 events were at ~25 °C (~55% RH), and the last 5 events were at ~20 °C (~53% RH) on a different date.

Mean for each method is the arithmetic average for the 13 events.

For the concentrations tested and the conditions under which the tests were performed, from Figure 4.18, it was generally observed that the average of MOS sensors measured ammonia concentrations calculated by both individual and unified equation were close to acid scrubbers. Acid scrubbers are highly accurate for ammonia concentrations measurements and have been widely used in monitoring poultry house air quality and exhaust (Shah et al., 2013, 2014). While the Drager EC sensors have been used for monitoring ammonia concentrations in poultry houses, they can be rapidly saturated and thus, require frequent purging (Shah et al., 2008).

Quantitative comparison of the average measurements made by the three methods are presented in Table 4.1. The unified (eq. [4.7]) and individual equations (eq. [4.4]-[4.6]) resulted in very similar RE and CV values (Table 4.1) which could be attributed to the relatively low RH (50-60%) of the exhaust gas from the poultry litter chamber. If RH had been higher, difference between the mean MOS-AVG and mean MOS\_UNI could have been higher. Similarly, RE and CV values of MOS\_AVG would have been higher (Table 4.1). This is because the RH1 sensor under-measured RH at  $\geq 80\%$  (Fig. 4.13) and this would have resulted in under-measurement by MOS1 (using eq. [4.4]). While compensation equation for RH and temperature were satisfactory, better quality RH and temperature sensors would allow using unified equation which will make the commercialization application more practical compare with developing compensation equations for individual sensor packages.

Table 4.1. Quantitative comparison of the three ammonia measurement methods (Drager, scrubber, and MOS/TGS2444 sensor units).

Measurements and parameters	Events <sup>1</sup>													
	1	2	3	4	5	6	7	8	9	10	11	12	13	Mean
<b>Scrubber conc. (ppm)</b>	49.3	39.5	23.6	18.1	36.3	34.2	31.3	23.1	12.2	14	11.4	10.5	18.3	24.8
<b>Drager EC sensor (ppm)</b>	41	31	14	10	28	37	35	16	7	8	5	5	11	19.1
<b>MOS sensor mean<sup>2</sup> (ppm)</b>	51	40	20	16	38	34	32	21	14	15	12	12	20	25
<b>MOS sensor SD (ppm)</b>	3.5	1.5	1.5	0.9	1.6	1.5	2.5	1.6	1.2	1.3	1.1	0.9	0.6	1.5
<b>MOS sensor CV<sup>3</sup> (%)</b>	4.4	6.8	6.5	4.5	4.9	6.7	6.2	7.0	11.9	12.6	9.2	9.2	8.8	7.6
<b>Unified MOS sensor mean<sup>4</sup> (ppm)</b>	53.3	41.4	20.8	16.9	38.8	35.1	35.1	22.0	10.8	12.2	9.7	9.7	16.6	24.9
<b>Unified MOS sensor SD (ppm)</b>	2.3	2.8	1.3	0.8	1.9	2.4	2.2	1.6	1.3	1.5	0.9	0.9	1.5	1.6
<b>Unified MOS sensor CV (%)</b>	4.4	6.8	6.5	4.5	4.9	6.7	6.2	7.0	11.9	12.6	9.2	9.2	8.8	7.6
<b>Relative error<sup>5</sup> of MOS vs. scrubber, %</b>	5.5	2.7	14.3	10.3	4.5	3.2	6.6	9.7	10.8	9.4	7.5	13.6	9.0	8.2
<b>Relative error of Drager vs. scrubber, %</b>	16.9	21.5	40.6	44.7	22.9	8.1	11.6	30.6	42.7	42.7	56.0	52.3	40.0	33.1
<b>Relative error of Unified MOS vs. scrubber, %</b>	8.0	6.8	11.8	6.3	6.8	6.2	12.1	6.0	11.9	12.7	14.6	7.4	9.7	9.2

<sup>1</sup>Each event was 10 min; <sup>2</sup>Mean of three MOS sensor readings calculated by individual equation, each sensor reading being the average of 120 measurements made every 5 s; <sup>3</sup>Coefficient of variation (n = 3) = SD/mean; <sup>4</sup>Mean of three MOS sensor readings calculated by unified equation; <sup>5</sup>RE or Inaccuracy = absolute (scrubber conc. – MOS or Drager conc.)\*100/Scrubber conc.

From Table 4.1 it is clear that with suitable RH and temperature compensation, the MOS sensor was more accurate than the Drager EC sensor. For research grade sensors, RE and CV of  $\leq 10\%$  are considered acceptable (Colls, 2002). When using individual compensation equations, in four out of 13 events, the MOS sensor's RE exceeded 10% (Table 4.1). For reference, the RE of color detector tubes commonly used in poultry houses is higher ( $\pm 15\text{-}18\%$  for  $\leq 50$  ppm) (RAE Systems, 2001). From Table 4.1, averaged over all the events, RE and CV of MOS sensor's readings calculated based on unified equation were also within the acceptable range of research grade sensor, which showed that using the unified equation could be valid. Comparison between the fabricated MOS sensor unit and color detector tube is presented in section 4.1.4. As also mentioned earlier, better quality RH and temperature sensors could have improved performance of the unified equation. After all, if this technology is commercialized, developing a unified equation for a batch of sensor packages will be more feasible than individual compensation equations.

Kawashima and Yonemura (2001) compared MOS sensors with boric acid scrubbers to measure ambient ammonia concentrations (10 ppb range). The MOS sensors had an error of  $\pm 9.7$  ppb (Kawashima and Yonemura, 2001) but since the targeted measurement range is under ppm level, it is not possible to directly compare our results with their study. Pecun and Zabloudivova (2009) compared the MOS sensor FIS SP-53 (similar to FIS SP-53B evaluated in this study) with the photoacoustic sensor for measuring ammonia concentrations from wood shavings spiked with ammonia and water. Compared with the photoacoustic sensor, the MOS sensors overestimated ammonia concentrations by 2.2 to 2.8 times (Pecun and Zabloudivova, 2009). Gates et al. (2005) developed a portable monitoring unit (PMU) which used an EC sensor (similar to Drager EC sensor evaluated in this study) to measure ammonia, comparison has been provided in Table 4.1 and Figure 4.17.

#### 4.1.4 Testing of the assembled units

Three fabricated units (namely, UNIT1, UNIT2, and UNIT3) were tested using air exhausted from a chamber containing poultry litter at ~20 °C and 60% RH for 4 h (Fig. 4.19). The three MOS sensors used their individual compensation equations (eq. [4.4]-[4.6]) and their outputs were noted manually. So, the unified equation (eq. [4.7]) could not be applied to the three sensors retroactively. The Drager EC sensor and gas tube were used for comparison purposes. It should also be noted that the EC sensor and gas tube are less accurate than the scrubber and so they cannot be considered to be ‘standard’ methods. It took more than 30 min for the water bath to heat the air used for testing the MOS sensors from room temperature (19-20 °C) to a higher temperature range of 30-32 °C. Further, as mentioned in Section 3.4, due to the limited heating capacity of the system, the three units were not tested simultaneously. Further, each gas tube measurement took 90 s. So the readings of the three MOS units cannot be considered to be replicates.

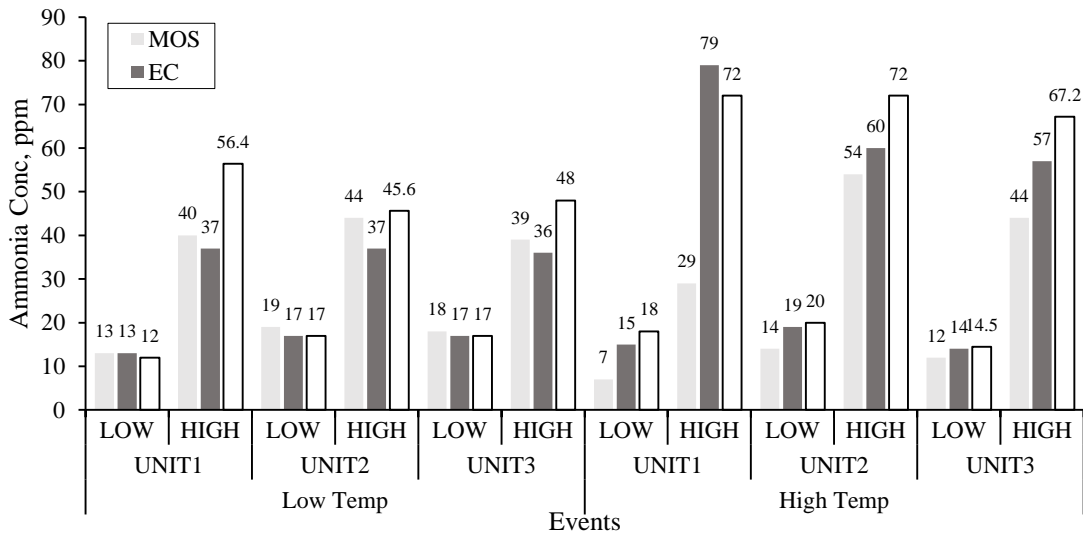


Figure 4.17. Comparison of ammonia concentrations in air exhausted from a chamber containing poultry litter measured with MOS sensor units, Drager EC sensor, and gas tube at 20 °C (58-63% RH) and 30 °C (40-45% RH). For each event, average Drager ammonia concentration is based on 10 readings while the average reading for each MOS sensor is based on 15 readings. The MOS sensors used their individual compensation equations.

In the low temperature testing, all three measurement methods gave very good agreement with the mean output of the MOS being within <7% of the grand mean of the three methods (Table 4.2). However, in the high temperature testing, agreement among the measurement methods was greatly reduced with the mean MOS measurement lower by >25% compared to the grand mean of the three methods (Table 4.3). The outputs of UNIT1 were much lower than the other MOS sensors as well as the EC and gas tube readings in the high temperature test (Fig. 4.18). This might be due to the poor-performance of UNIT1’s RH sensor but it is unclear why ammonia concentrations at low temperature were similar to those of UNIT2 and UNIT3. So, as will be discussed later, UNIT1’s RH sensor was replaced.

Table 4.2. Comparison of the mean of the three MOS sensor units’ output with the grand mean of three ammonia measurement methods (MOS/TGS2444 sensor units, Drager EC sensor, and gas tube) for each of the test conditions presented in Fig. 4.18.

	Low temp Low conc.	Low temp High conc.	High temp Low conc.	High temp High conc.
Grand mean <sup>1</sup>	16	43	15	59
MOS mean <sup>2</sup>	17	41	11	42
Difference <sup>3</sup> (%)	6.3	4.7	26.7	28.8

<sup>1</sup>Grand mean of the average readings of three methods for each test condition; <sup>2</sup>MOS mean is based on the readings of three MOS sensor units; <sup>3</sup> Difference = absolute (MOS mean – Grand mean)\*100/ Grand mean.

The original RH sensor in UNIT3 was damaged during fabrication of the unit and had to be replaced; the defective RH1 sensor was also replaced. However, the new RH sensor installed in UNIT3 was not tested to see how an untested RH sensor would perform. As will be discussed later, there was good agreement between UNIT2 and UNIT3.

After replacing the RH sensors in UNIT1 and UNIT3, the three MOS sensor units were tested again by comparing with Drager EC sensor in the high temperature range (30-32 °C) at five different ammonia levels sequentially (Fig. 4.20). As mentioned earlier, the three temperature (Fig. 4.14) and three ammonia (Fig. 4.12) sensors’ readings were close to one-

another; therefore, the equation for UNIT2 was used in UNIT1 and UNIT3 after the two RH sensors were replaced. The average difference in measurement between the Drager EC sensor (37 ppm) and the average output of the three MOS sensors (35 ppm) was ~5% (Fig. 4.20), showing that there was good agreement between the two methods even under high temperatures when the faulty RH sensors were replaced in UNIT1 and UNIT3.

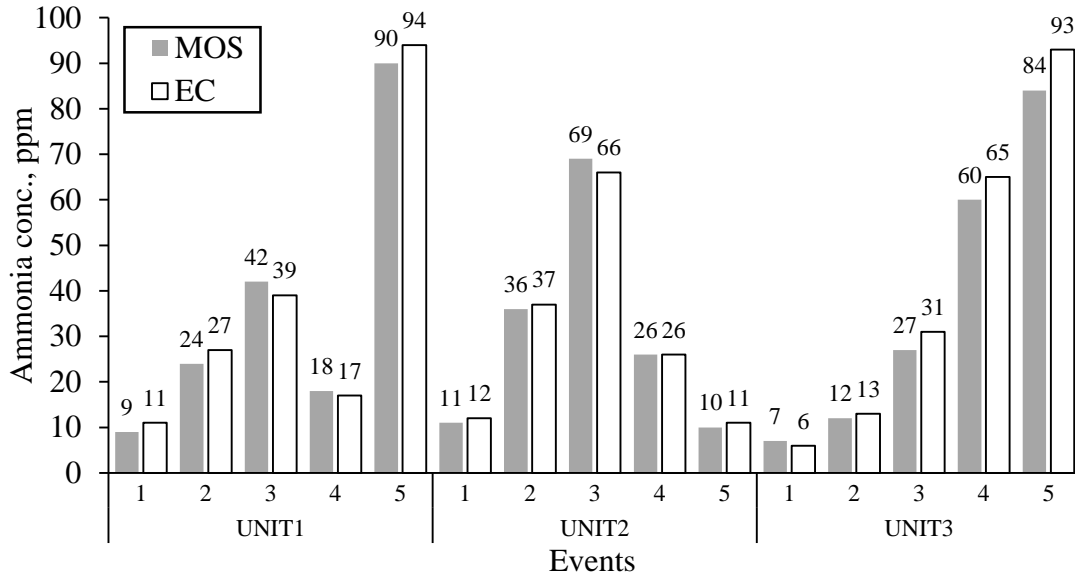


Figure 4.18. Comparison of poultry litter exhaust air ammonia concentrations measured with MOS sensor units and Drager EC sensor at 30 °C. Drager ammonia concentration is based on 10 readings while the average reading for each MOS sensor is based on 15 readings. All MOS sensors used eq. [4.5] for temperature and RH compensation. The average reading for the three MOS sensor units and EC sensor is 35 and 37 ppm, respectively.

Results presented in Figure 4.20 indicated that upon replacement of the defective RH sensors, use of the temperature and RH compensation equations greatly reduced the difference in outputs between the MOS sensors and the Drager EC sensor even at high temperatures. The accuracy of the RH compensation equation had been confirmed earlier by comparison with the boric acid scrubber results at lower temperatures (Fig. 4.18).

*Post-hoc*, one MOS sensor unit (UNIT2) was compared with the Drager sensor under

changing temperature conditions (Fig. 4.21). Interestingly, during the first four events that was conducted over 30 min, as the temperature decreased from 30.2 °C to 24.5 °C, the difference in output between the two methods continued to increase (Fig. 4.21). When the Drager EC sensor was replaced with another Drager EC sensor that had been previously purged, for the last four events that took about 15 min, as the temperature decreased from 24.5 °C to 22.1 °C, the two methods gave similar readings. Hence, it seemed that the Drager EC sensor required more frequent purging than the MOS sensor.

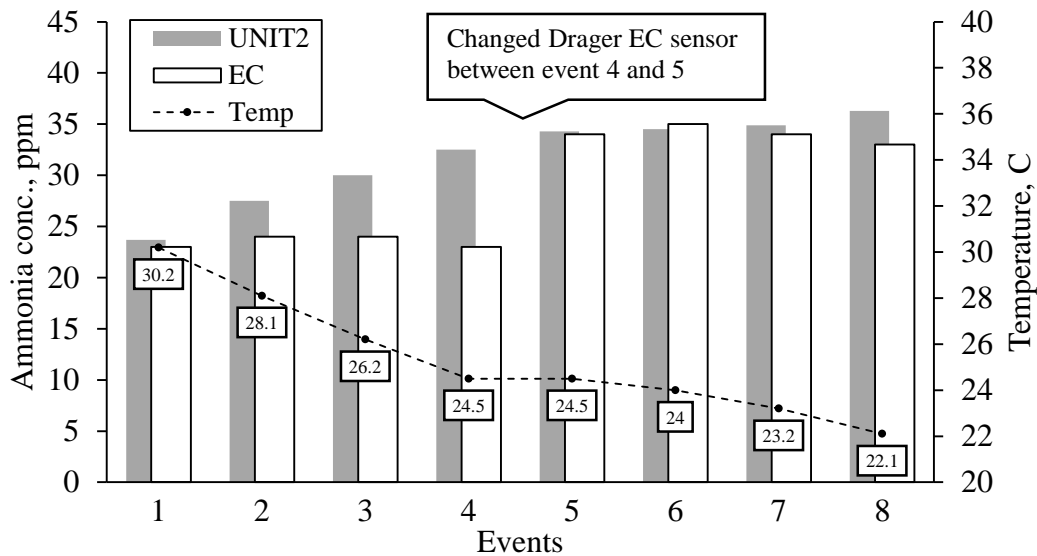


Figure 4.19. Comparison of ammonia concentrations in air exhausted from a chamber containing poultry litter measured with MOS sensor unit (UNIT2, eq. [4.4]) and Drager EC sensor under changing temperature conditions from 20 °C (57% RH) to 30 °C (30% RH).

Drager ammonia concentration is on the average of 10 readings while the MOS sensor concentration is on the average of 15 readings.

Based on the results presented in Fig. 4.17 and Table 4.1, the MOS sensors displayed acceptable accuracy and variability. Accuracy of some stationary research quality measurement method such as, FTIR, PAS, and DOAS range between 3% and 11% (Zwicker et al., 1998; PAAQL, 2007; Myers et al., 2000). Among portable devices, the pH test paper has an accuracy of  $\pm 20\%$  (Moum et al., 1969), the Drager EC sensor was reported to have an

accuracy of  $\pm 3\%$ , and RAE Systems (2001) reported that their gas tubes had an accuracy of  $\pm 10$  and  $18\%$ . Hence, with temperature and RH compensation, the TGS2444 sensors gave higher accuracies than the management-type portable methods used in this study.

#### 4.2. Oxygen sensor testing

Two oxygen sensors, namely, KE25 and SGX4 were calibrated under fixed RH and temperature conditions. Three oxygen concentrations ( $\sim 17$ ,  $\sim 19$ , and  $\sim 21\%$ ) were used. The sensors' voltage outputs increased linearly with oxygen concentration as shown in eq. [4.8] and eq. [4.9].

$$\text{KE25:} \quad [O_2] = 28.9 * V_{\text{KE25}} + 6.3 \quad [4.8]$$

$$\text{SGX4:} \quad [O_2] = 22.7 * V_{\text{SGX4}} + 3.8 \quad [4.9]$$

In equations [4.8] and [4.9],  $[O_2]$  is oxygen concentration (%);  $V_{\text{KE25}}$  is the KE25 sensor's voltage output (V); and  $V_{\text{SGX4}}$  is the SGX4 sensor's voltage output (V).

As shown in Figures 4.22, the two sensor exhibited low relative error ( $< 0.4\%$ ) when compared with calculated oxygen concentration.

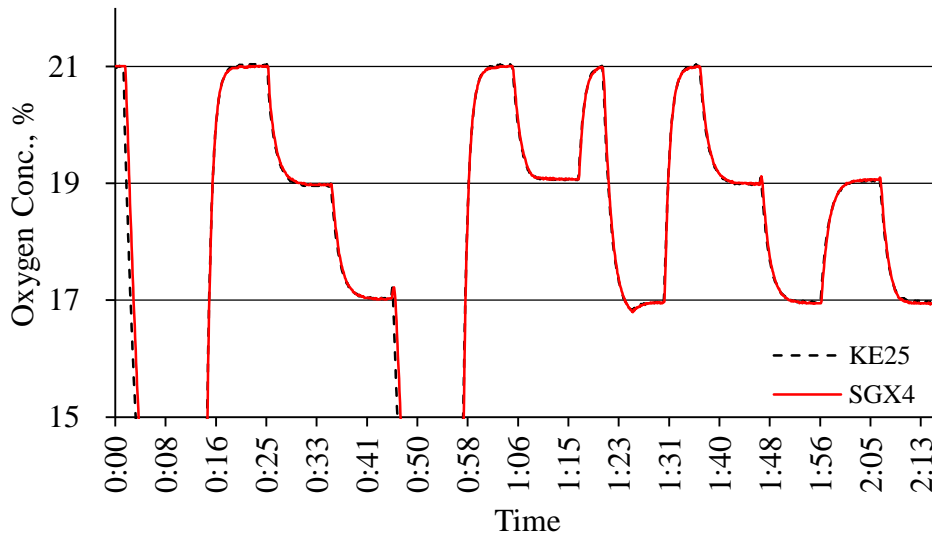


Figure 4.20. Responses of one KE25 and one SGX4 sensor to 17, 19, and 21% oxygen concentration at 43% RH and 25.1 °C. Measurements were made every 5 s.

To evaluate the impact of RH, the two oxygen sensors were exposed to dry ( $\sim 18\%$ ) and

highly humidified (~82%) air (Fig 4.21). With no RH compensation, the KE25 sensor's readings decreased 0.8% at each oxygen concentration level, whereas the SGX4 sensor's outputs decreased by 1.3%. The KE25 oxygen sensor seemed to perform slightly better than the SGX4 sensor; moreover, the life time of the SGX4 sensor is only 2 yr compared with 5 yr for the KE25 sensor. Hence, despite being more expensive Figaro KE25 sensor was selected for use in the sensor system. While this was not a replicated study, the KE-25 sensor has been in use for several decades and has been evaluated in several studies (e.g., Shum et al., 2011; Bower et al., 2000; Flodin et al., 1999.).

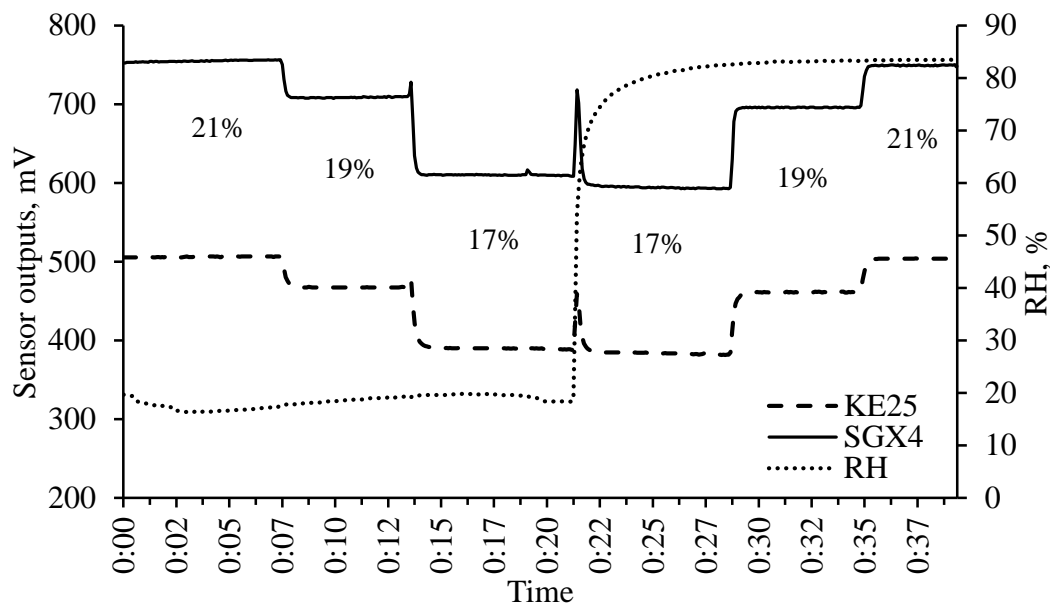


Figure 4.21. Responses of one SGX4 and one KE25 sensor to 17, 19, and 21% oxygen at high (~80%) and low (~18%) RH condition. Measurements were made every 5 s.

After calibration, the three KE25 oxygen sensors were installed alongside the MOS sensor units, and then tested in the ambient environment (oxygen concentration of ~20.9%) (Table 4.4). The temperature and RH sensor readings in this test varied among one-another. Due to the relatively stable response of the oxygen sensor, no further tests were conducted. The three units' average oxygen reading under the ambient condition was 20.9%, and the standard deviation was <0.1%. Research on the use of oxygen sensors in the poultry house

could not be located to compare the findings of this study with other published research.

Table 4.2. Responses of the three oxygen sensors and their respective RH and temperature sensors to ambient condition (30.3-30.8 °C and 37.5-50.1% RH). Ambient temperature and RH were measured with a TMA40-A anemometer equipped with temperature and RH sensors.

Time	UNIT1			UNIT2			UNIT3		
	O <sub>2</sub> Conc. (%)	RH (%)	Temp (°C)	O <sub>2</sub> Conc. (%)	RH (%)	Temp (°C)	O <sub>2</sub> Conc. (%)	RH (%)	Temp (°C)
15:39	20.9	48.7	32.2	20.9	42.7	31.1	21	50.1	30.8
15:42	20.9	48.7	33.0	20.9	42.1	31.6	21	49.1	30.8
15:44	20.9	46.3	33.6	20.9	39.5	32.4	21	47	31.3
15:47	20.9	45.3	34.1	20.9	38.4	33	20.9	46.5	31.6
15:49	20.9	44	34.4	20.9	38	33	21	45.7	31.9
15:51	20.9	44	34.7	20.9	37.5	33.2	21	45.3	31.9
<b>Average oxygen reading</b>								20.9%	
<b>Standard deviation</b>								<0.1%	

Because these three units are hand-made prototypes, there is scope for improvement. For example, the location of RH and temperature sensor to the heating components (vacuum pump or circuit board) could influence the RH and temperature of the air sample, especially when the unit is operated for long periods. Further tests with more replicates is needed both, in the lab and in poultry houses. There is need to convert this consider conversion of this device to operate in a diffusive mode; this could reduce the price, mass, and complexity of the system.

## 5. Conclusions and Recommendations for Future Work

Research has shown that high ammonia concentrations and low oxygen concentrations can reduce bird performance. There is need for low-cost and portable sensors that can be used to monitor ammonia and oxygen levels in poultry houses. Currently, portable ammonia measurement methods used in poultry houses include pH test paper, gas tube, and EC sensor; while these methods have advantages but they also have drawbacks that limit their adoption. A low-cost and portable ammonia – oxygen sensor system would fulfill an important need. An MOS ammonia sensor and EC oxygen sensor which are both low-cost, compact in size, and have long lives, may be suitable for such as a sensor system. Three brands of MOS ammonia sensors and two brands of oxygen sensors were compared using synthetic gas mixtures, and one sensor was selected for each gas. Due to the influence of moisture and temperature on the MOS ammonia sensor, these parameters were measured with low-cost RH and temperature sensor collocated with the selected MOS ammonia sensor. Thereafter, the impacts of these parameters were accounted for by using a multiple linear regression-based compensation equation. The ammonia sensor unit was tested under different conditions and also compared with other ammonia measurement methods. The ammonia sensor unit and oxygen sensor were packaged and were further tested. Findings of this study are listed below.

- The Figaro TGS2444 ammonia sensor was selected because of its rapid response time and low ammonia concentration  $\times$  RH interaction characteristic.
- The KE25 oxygen sensor was selected due to its lower sensitivity to moisture and longer life.
- The TGS2444 sensor had a low response time and low short-term drift, permitting its continuous use for up to 40 min without purging.
- The compensation equations were effective in accounting for the effects of RH and temperature on sensor response. Display of the temperature and RH readings will enhance the utility of the sensor system.
- Variabilities among the RH and temperature sensor influenced the accuracy of the sensing system.
- Three units of the sensor system tested with ammonia laden gas mixture exhausted from

a poultry litter chamber showed that the system had an average RE of 8.2% and an average CV of 6.6% when individual RH compensation equations were used for the sensors. Even the use of a unified equation changed RE and CV only slightly.

- Other gases present in the air exhausted from the chamber containing poultry litter likely did not affect the ammonia sensor's performance.
- The total mass of the sensor unit was <1.4 Kg with a material cost of <\$450.

Based on this work, following are the recommendations for future work.

- Consider development of the MOS system for use in diffusive mode to reduce cost and improve portability.
- More accurate RH and temperature sensors should be evaluated to see if they can improve the system's accuracy for research grade application.
- There is need for additional testing of the sensor system in poultry houses.

## REFERENCES

- Adams, R. P. 2007. Identification of essential oil components by gas chromatography/mass spectrometry (No. Ed. 4). Allured Publishing Corporation.
- AIHA. 1993. Direct-Reading Colorimetric Indicator Tubes Manual, 2nd. Ed. Publication No. 172-SI-93. Falls Church, VA: Am. Industrial Hygiene Assoc.
- American Humane Association. 2012. Animal welfare standard for broiler chickens. Available at: [www.humaneheartland.org/our-standards](http://www.humaneheartland.org/our-standards). Accessed 10 August 2015.
- Aneja, V. P., E. P. Stahel, H. H. Rogers, A. M. Witherspoon, and W. W. Heck. 1978. Calibration and performance of a thermal converter in the continuous atmospheric monitoring of ammonia. *Analytical Chemistry*, 50(12), 1705-1708.
- Arshak, K., E. Moore, G. M. Lyons, J. Harris, and S. Clifford. 2004. A review of gas sensors employed in electronic nose applications. *Sensor Review*, 24(2), 181-198.
- Aviagen. 2009. Effective management practices to reduce the incidence of ascites in broilers. Available at: [www.aviagen.com](http://www.aviagen.com). Accessed 10 August 2015.
- Aziz, T., and H. J. Barnes. 2010. Harmful effects of ammonia on birds. *World Poultry*, 26(3), 28-30.
- Barsan, N., and U. Weimar. 2001. Conduction model of metal oxide gas sensors. *Journal of Electroceramics*, 7(3), 143-167.
- Barsan, N., and U. Weimar. 2003. Understanding the fundamental principles of metal oxide based gas sensors; the example of CO sensing with SnO<sub>2</sub> sensors in the presence of humidity. *Journal of Physics: Condensed Matter*, 15(20), R813.
- Bedford, G., and J. H. Thomas. 1972. Reaction between ammonia and nitrogen dioxide. *Journal of the Chemical Society, Faraday Transactions 1: Physical Chemistry in Condensed Phases*, 68, 2163-2170.
- Besch, E. L., and H. Kadono. 1978. *Cardiopulmonary responses to acute hypoxia in domestic fowl. Respiratory function in birds, Adult and Embryonic*. Springer Berlin Heidelberg. Berlin, Germany.
- Bicudo, J. R., C. L. Tengman, L. D. Jacobson, and J. E. Sullivan. 2000. Odor, hydrogen sulfide and ammonia emissions from swine farms in Minnesota. *Proceedings of the*

- Water Environment Federation, 2000(3), 589-608.
- Blake, J. P., and Hess, J. B. 2001. Sodium bisulfate as a litter treatment, ANR-1208. Alabama Cooperative Extension System.
- Blanes-Vidal, V., M. N. Hansen, S. Pedersen, and H. B. Rom. 2008. Emissions of ammonia, methane and nitrous oxide from pig houses and slurry: Effects of rooting material, animal activity and ventilation flow. *Agriculture, Ecosystems and Environment*, 124(3), 237-244.
- Bower, J., B. D. Patterson, and J. J. Jobling. 2000. Permeance to oxygen of detached *Capsicum annuum* fruit. *Animal Production Science*, 40(3), 457-463.
- Brattain, W. H., and J. Bardeen. (1953). Surface properties of germanium. *Bell System Technical Journal*, 32(1), 1-41.
- Brunsch, R. (1997). Methodical aspects relating the results of multigas monitoring and multipoint sampling. In *Ammonia and Odour Control from Animal Production Facilities. Proceedings of the International Symposium*. (Vol. 1, pp. 185-191).
- COBB. 2008. *Broiler Management Guide*.
- Czarick, M. and B. Fairchild. 2002. Measuring ammonia levels in poultry houses. *Poultry Housing Tips* 14(8). Univ. of Georgia Cooperative Extension Service.
- Czarick, M., and Fairchild, B. 2002. Running timer fans prior to chick placement. *Poultry Housing Tips*, 14(3). Univ. of Georgia Cooperative Extension Service.
- EMEP. 2001. *EMEP Manual for Sampling and Chemical Analysis*, Rep. No. EMEP/CCC-1/95. Norwegian Institute for Air Research Kjeller, Norway.
- EPA. 2004. *National emission inventory — Ammonia emissions from animal husbandry*. Available at:  
[http://www.epa.gov/ttn/chief/ap42/ch09/related/nh3inventoryfactsheet\\_jan2004.pdf](http://www.epa.gov/ttn/chief/ap42/ch09/related/nh3inventoryfactsheet_jan2004.pdf). Accessed Jul. 2004.
- Ferm, M., T. Marcinkowski, M. Kieronczyk, and S. Pietrzak. 2005. Measurements of ammonia emissions from manure storing and spreading stages in Polish commercial farms. *Atmospheric Environment*, 39(37), 7106-7113.
- Fierro, J. L. G. 2010. *Metal oxides: chemistry and applications*. CRC press.

- Figaro. 2005. General information for TGS sensors. Osaka, Japan.
- Figaro. 2006. Evaluation Module for TGS2444-EM2444. Osaka, Japan.
- Figaro. 2012. Technical information for TGS2444. Osaka, Japan.
- Fitz, D. R., J. T. Pisano, I. L. Malkina, D. Goorahoo, and C. F. Krauter. 2003. A passive flux denuder for evaluating emissions of ammonia at a dairy farm. *Journal of the Air & Waste Management Association*, 53(8), 937-945.
- Flodin, C., J. H. Bower, and B. D. Patterson. 1999. Oxygen permeance: a method applied to modified atmosphere packages containing fresh plant foods. *Packaging Technology and Science*, 12(4), 185-191.
- Galloway, J. N. 1998. The global nitrogen cycle: changes and consequences. *Environmental pollution*, 102(1), 15-24.
- Gates, R.S., H. Xin, K.D. Casey, Y. Liang, and E.F. Wheeler. 2005. Method for measuring ammonia emissions from poultry houses. *The Journal of Applied Poultry Research*, 14(3), 622-634.
- Gerber, P., Opio, C., and Steinfeld, H. (2007). Poultry production and the environment—a review. Available at:  
[http://www.fao.org/Ag/againfo/home/events/bangkok2007/docs/part2/2\\_2.pdf](http://www.fao.org/Ag/againfo/home/events/bangkok2007/docs/part2/2_2.pdf). Accessed 18 August 2015.
- Gong, J., Q. Chen, M. Lian, N. Liu, R.G. Stevenson, and F. Adamic. 2006. Micromachined Nanocrystalline Silver Doped SnO<sub>2</sub> H<sub>2</sub>S Sensor. *Sensors and Actuators B: Chemical*, 114(1), 32-39.
- Grob, R. L., and E. F. Barry. 2004. *Modern practice of gas chromatography*. John Wiley and Sons.
- Kauffman, D. R., and A. Star. 2008. Carbon nanotube gas and vapor sensors. *Angewandte Chemie International Edition*, 47(35), 6550-6570.
- Hanrahan, G., D. G. Patil, and J. Wang. 2004. Electrochemical sensors for environmental monitoring: design, development and applications. *Journal of Environmental Monitoring*, 6(8), 657-664.
- Harris, D. B., R. C. Shores, and L. G. Jones. 2001. Ammonia emission factors from swine

finishing operations. United States Environmental Protection Agency, Office of Research and Development, National Risk Management Research Laboratory, Research Triangle Park, NC.

Heiland, G., D. Kojl, and T. Seiyama. 1988. Chemical sensor technology (Vol. 2). Elsevier.

Heldman, D. R., and C. I. Moraru. 2003. Encyclopedia of agricultural, food, and biological engineering. Marcel Dekker. New York City

Henrich, V.E., and P. A. Cox. (1996). The surface science of metal oxides. Cambridge University Press. Cambridge, United Kingdom.

Hu, X., T. Norimichi, K. Masaru, B. Hiroshi, and M. Yasuaki. 2012. Mechanism of chemiluminescence reaction between hypobromite and ammonia or urea. Bulletin of the Chemical Society of Japan, 69(5), 1179-1185.

Ihokura, K., and J. Watson. 1994. The Stannic Oxide Gas Sensor Principles and Applications. CRC Press. Boca Raton, Florida.

Jia, M., J. Koziel, and J. Pawliszyn. 2000. Fast field sampling/sample preparation and quantification of volatile organic compounds in indoor air by solid - phase microextraction and portable gas chromatography. Field Analytical Chemistry & Technology, 4(2-3), 73-84.

Kamin, H., J. C. Barber, S. I. Brown, C. C. Delwiche, D. Grosjean, J. M. Hales, ... and J. A. Frazier. 1979. Ammonia. University Park Press, Baltimore.

Kawashima, S. and S. Yonemura. 2001. Measuring ammonia concentration over a grassland near livestock facilities using a semiconductor ammonia sensor. Atmospheric Environment, 35(22), 3831-3839.

Lumense. 2013. Lumense ammonia monitor. Available at: [www.lumense.com](http://www.lumense.com). Accessed 10 August 2015.

Manning, A. C., R. F. Keeling, and J. P. Severinghaus. 1999. Precise atmospheric oxygen measurements with a paramagnetic oxygen analyzer. Global Biogeochemical Cycles, 13(4), 1107-1115.

McCulloch, R. B., and A. D. Shendrikar. 2000. Concurrent atmospheric ammonia measurements using citric-acid-coated diffusion denuders and a chemiluminescence

- analyzer. *Atmospheric Environment*, 34(28), 4957-4958.
- Meyer, V. M., and D. S. Bundy. 1991. Farrowing building air quality survey. Paper-American Society of Agricultural Engineers (USA). Paper No. 914012.
- Miles, D. M., S. L. Branton, and B. D. Lott. 2004. Atmospheric ammonia is detrimental to the performance of modern commercial broilers. *Poultry Science*, 83(10), 1650-1654.
- Mizsei, J. 1995. How can sensitive and selective semiconductor gas sensors be made. *Sensors and Actuators B: Chemical*, 23(2), 173-176.
- Mosquera, J., P. Hofschreuder, and A. Hensen. (2002). Application of new measurement techniques and strategies to measure ammonia emissions from agricultural activities, IMAG Rapport 2002-11, Wageningen, The Netherlands.
- Moum, S. G., W. Seltzer, and T. M. Goldhaft. 1969. A simple method of determining concentrations of ammonia in animal quarters. *Poultry Science*, 48(1), 347-348.
- Myers, J., T. Kelly, C. Lawrie, and K. Riggs. 2000. Environmental Technology Verification Report: Opsi Inc. AR-500 Ultraviolet Open-Path Monitor. Battelle Columbus, Ohio
- Nanto, H., T. Minami, and S. Takata. 1986. Zinc-oxide thin-film ammonia gas sensors with high sensitivity and excellent selectivity. *Journal of Applied Physics*, 60(2), 482-484.
- National Chicken Council. 2014. Animal welfare guidelines and audit checklist. Available at: [www.nationalchickencouncil.org](http://www.nationalchickencouncil.org). Accessed 10 August 2015.
- National Institute for Occupational Safety and Health. 1992. Occupational safety health guideline for ammonia. Available at: [www.cdc.gov](http://www.cdc.gov). Accessed 10 August 2015.
- New York State Department of Health. 2004. The facts about ammonia. Available at: [http://www.health.ny.gov/environmental/emergency/chemical\\_terrorism/ammonia\\_tech.htm](http://www.health.ny.gov/environmental/emergency/chemical_terrorism/ammonia_tech.htm). Accessed 16 August 2015.
- Occupational Health and Safety. 2005. Understanding oxygen sensor performance. Available at: <http://ohsonline.com/Articles/2005/05/Understanding-Oxygen-Sensor-Performance.aspx>. Accessed 16 August 2015.
- Osada, T., H. B. Rom, and P. Dahl. 1998. Continuous measurement of nitrous oxide and methane emission in pig units by infrared photoacoustic detection. *Transactions of the ASAE*, 41(4), 1109-1114.

- Ott, L., M. Longnecker, and R. L. Ott. 2001. *An Introduction to Statistical Methods and Data Analysis* (Vol. 511). Duxbury Press. Pacific Grove. CA.
- Pearce, T. C., S. S. Schiffman, H. T. Nagle, and J. W. Gardner. 2006. *Handbook of Machine Olfaction: Electronic Nose Technology*. John Wiley and Sons.
- Pecen, J. and P. Zabloudilova. 2005. The comparison of two types' sensors for ammonia emission continual measurement. *Research in Agricultural Engineering*, 51:112-118.
- Peng, X. (2012) Nanowires – recent advances. InTech, Chapters published
- Philippe, F. X., J. F. Cabaraux, and B. Nicks. 2011. Ammonia emissions from pig houses: Influencing factors and mitigation techniques. *Agriculture, ecosystems & environment*, 141(3), 245-260.
- Phumman, P., S. Niamlang, and A. Sirivat. 2009. Fabrication of poly (p-phenylene)/zeolite composites and their responses towards ammonia. *Sensors*, 9(10), 8031-8046.
- Ramamoorthy, R., P. K. Dutta, & S. A. Akbar. 2003. Oxygen sensors: materials, methods, designs and applications. *Journal of Materials Science*, 38(21), 4271-4282.
- Ricco, A. J., S. J. Martin, and T. E. Zipperian. 1985. Surface acoustic wave gas sensor based on film conductivity changes. *Sensors and Actuators*, 8(4), 319-333.
- Ross, J. F., I. Robins, and B. C. Webb. 1987. The ammonia sensitivity of platinum-gate MOSFET devices: dependence on gate electrode morphology. *Sensors and Actuators*, 11(1), 73-90.
- RAE Systems. 2001. *Gas Detection Tubes and Sampling Handbook*. Available at: [www.raesystems.com](http://www.raesystems.com). Accessed 10 August 2015.
- Santra, S., A. K. Sinha, S. K. Ray, Syed Z. Ali, Florin Udrea, J. W. Gardner and P. K. Guha. 2014. Ambient temperature carbon nanotube ammonia sensor on CMOS platform. *Procedia Engineering*, 87, 224-227.
- Sarkar, D., H. Gossner, W. Hansch, and K. Banerjee. 2013. Tunnel-field-effect-transistor based gas-sensor: Introducing gas detection with a quantum-mechanical transducer. *Applied Physics Letters*, 102(2), 023110.
- SAS. 2012. *User's Guide*. Version 9.3. Cary, N.C.: SAS Institute.
- Sather, M. E., J. Mathew, N. Nguyen, J. Lay, G. Golod, R. Vet, and F. Geasland 2008.

- Baseline ambient gaseous ammonia concentrations in the Four Corners area and eastern Oklahoma, USA. *Journal of Environmental Monitoring*, 10(11), 1319-1325.
- Secrest, C. D. (2001). Field measurement of air pollutants near swine confined-animal feeding operations using UV DOAS and FTIR. In *Environmental and Industrial Sensing* (pp. 98-104). International Society for Optics and Photonics.
- Seifert, R., B. K. Hubert, F. Kevin, and K. Heinz. 2009. Efficient Calibration and Recalibration of Metal Oxide Gas Sensors by a New Mathematical Procedure. *SENSOR+TEST Conference 2009*.
- Shah, S.B., Westerman, P. W., and Arogo, J. 2006. Measuring ammonia concentrations and emissions from agricultural land and liquid surfaces: a review. *Journal of the Air and Waste Management Association*, 56(7), 945-960.
- Shah, S.B., C.L. Baird, T.K. Marshall, P.W. Westerman, E.P. Harris, E. Oviedo-Rondon, J. Grimes, T. Marsh-Johnson, D. Campeau, M. Adcock, R. Munilla, H. Yao, and J. Wiseman. 2008. Acidifier dosage impacts on ammonia concentrations and emissions from heavy-broiler houses. ASABE international meeting. Paper No. 083922. St. Joseph, MI: ASABE.
- Shah, S.B., E.O. Oviedo-Rondon, J.L. Grimes, P.W. Westerman, and D. Campeau. 2013. Acidifier dosage effects on inside ammonia concentrations in roaster houses. *Applied Engineering in Agriculture*. 29:573-580.
- Shah, S.B., J.L. Grimes, E.O. Oviedo-Rondon, and P.W. Westerman. 2014. Acidifier application rate impacts on ammonia emissions from US roaster chicken houses. *Atmospheric Environment*, 92:576-583.
- Sharma, S., Hussain, S., Singh, S., and Islam, S. S. 2014. MWCNT-conducting polymer composite based ammonia gas sensors: A new approach for complete recovery process. *Sensors and Actuators B: Chemical*, 194, 213-219.
- Shen, C. Y., C. P. Huang, and W. T. Huang. 2004. Gas-detecting properties of surface acoustic wave ammonia sensors. *Sensors and Actuators B: Chemical*, 101(1), 1-7.
- Shum, L. V., P. Rajalakshmi, A. Afonja, G. McPhillips, R. Binions, L. Cheng, and S. Hailes. 2011. On the Development of a Sensor Module for real-time Pollution Monitoring. In

- Information Science and Applications (ICISA), 2011 International Conference on (pp. 1-9). IEEE.
- Simon, I., N. Barsan, M. Bauer, and U. Weimar. 2001. Micromachined metal oxide gas sensors: opportunities to improve sensor performance. *Sensors and Actuators B: Chemical*, 73(1):1-26.
- Snell, H. G. J., F. Seipelt, and H. F. A. Van den Weghe. 2003. Ventilation rates and gaseous emissions from naturally ventilated dairy houses. *Biosystems Engineering*, 86(1), 67-73.
- Sohn, J. H., M. Atzeni, L. Zeller, and G. Pioggia. 2008. Characterisation of humidity dependence of a metal oxide semiconductor sensor array using partial least squares. *Sensors and Actuators B: Chemical*, 131(1), 230-235.
- Steinfeld, H., P. Gerber, T. Wassenaar, V. Castel, M. Rosales, & C. D. Haan. 2006. *Livestock's long shadow: environmental issues and options*. Food and Agriculture Organization of the United Nations (FAO).
- Stuart, B. 2005. *Infrared spectroscopy*. John Wiley & Sons, Inc. Hoboken, NJ.
- Suehiro, J., G. Zhou, and M. Hara. 2003. Fabrication of a carbon nanotube-based gas sensor using dielectrophoresis and its application for ammonia detection by impedance spectroscopy. *Journal of Physics D: Applied Physics*, 36(21), L109.
- Taguchi, N. 1971. U.S. Patent, 3, 436, 631.
- Tavoli, F., and A. Naader. 2012. Optical ammonia gas sensor based on nanostructure dye-doped polypyrrole. *Sensors and Actuators B: Chemical*, 176,761–767.
- Tury, E. L., K. Kaste, R. E. Johnson, and D. O. Danielson. 1991. U.S. Patent No. 5,060,505. Washington, DC: U.S. Patent and Trademark Office.
- USDA NASS. 2014. National agricultural statistics service. Available at: [www.nass.usda.gov](http://www.nass.usda.gov). Accessed 10 August 2015.
- Vallespi, A., S. Verónica, P. Alejandro, and S. Guillermo. 2013. CO<sub>2</sub> Laser-Based Pulsed Photoacoustic Ammonia Detection. *International Journal of Thermophysics*, 34,8-9.
- Vogel, J. A., & P. D. Sturkie. 1963. Cardiovascular responses of the chicken to seasonal and induced temperature changes. *Science* 140:1404–1406.
- Walsh, S.E. Gant, K.P. Dowker, and R. Batt. 2010. Response of electrochemical oxygen

- sensors to inert gas–air and carbon dioxide–air mixtures: Measurements and mathematical modelling, *Journal Hazardous Materials*, 186: 190–196.
- Wan, Q., Q. H. Li, Y. J. Chen, T. H. Wang, X. L. He, J. P. Li, and C. L. Lin. 2004. Fabrication and ethanol sensing characteristics of ZnO nanowire gas sensors. *Applied Physics Letters*, 84(18), 3654-3656.
- Wang, C., L. Yin, L. Zhang, D. Xiang, and R. Gao. 2010, Metal Oxide Gas Sensors: Sensitivity and Influencing Factors. *Sensors*, 10(3),2088-2106.
- Wang, X., J. Zhang, and Z. Zhu. 2006. Ammonia sensing characteristics of ZnO nanowires studied by quartz crystal microbalance. *Applied Surface Science*, 252(6), 2404-2411.
- Weppner, W. 1992. Advanced principles of sensors based on solid state ionics. *J. Materials Science and Engineering: B*, 15(1), 48-55.
- Wheeler, E. F., K. D. Casey, R. S. Gates, H. Xin, J. L. Zajackowski, P. A. Topper, ... and A. J. Pescatore. 2006. Ammonia emissions from twelve US broiler chicken houses. *Transactions of the ASAE*, 49(5), 1495.
- Wheeler, E.F., R.W. J. Weiss, and E. Weidenboerner. 2000. Evaluation of Instrumentation for Measuring Aerial Ammonia in Poultry Houses. *The Journal of Applied Poultry Research*, 9(4), 443-452.
- White, R. 1989. *Chromatography/Fourier transform infrared spectroscopy and its applications* (Vol. 10). CRC Press.
- Wyers, G. P., R. P. Otjes, and J. Slanina. 1993. A continuous-flow denuder for the measurement of ambient concentration and surface-exchange fluxes of ammonia.
- Yamazoe, N. 1991. New approaches for improving semiconductor gas sensors. *Sensors and Actuators B: Chemical*, 5(1), 7-19.
- Zhang, G., J. S. Strøm, B. Li, H. B. Rom, S. Morsing, P. Dahl, and C. Wang. 2005. Emission of ammonia and other contaminant gases from naturally ventilated dairy cattle buildings. *Biosystems Engineering*, 92(3), 355-364.
- Zhang, J. X., and K. Hoshino. 2013. *Molecular Sensors and Nanodevices: Principles, Designs and Applications in Biomedical Engineering*. William Andrew. Norwich, NY.
- Zhang, W., and Z. Lingjuan. 1989. The ammonia sensitivity of Pd-Ir alloy-gate mos field-

effect transistor. *Sensors and Actuators*, 19(2), 177-181.

Zhong, Q., H. Xu, H. Ding, L. Bai, Z. Mu, Z. Xie, ... and Z. Gu. 2013. Preparation of conducting polymer inverse opals and its application as ammonia sensor. *Colloids and Surfaces A: Physicochemical and Engineering Aspects*, 433, 59-63.

Zwicker, J.O., E. Ringler, and T. Waldron. 1998. OP-FTIR monitoring for ammonia emissions in the San Joaquin Valley. *Proceedings-spie the international society for optical engineering*, 3534: 150-161.